# Electron microscopic study using paraffin sections

In the diagnostic pathology practice, specimens for electron microscopy (EM) are not necessarily handled and fixed under the ideal condition. Ultrastructural study using formalin-fixed and/or paraffin-embedded material are described herein. The fine morphologic preservation is often acceptable, particularly when small cubes are dug out of paraffin blocks. Particulate structures such as neuroendocrine granules and microbes are consistently observed even using paraffin sections. Paraffin sections signalized with silver particles in Grimelius and Grocott stains or diaminobenzidine products in immunostaining and *in situ* hybridization can be applied to EM evaluation by using a pre-embedding sequence. The practical merit includes the targeted approach: highly accurate sampling from focal lesions can be achieved for EM analysis, after observing hematoxylin and eosin-stained or specific-signalized paraffin-sections. This allows us pathologists a convenient and practical way for identifying focally infected pathogens, as well as a retrospective ultrastructural analysis of rare lesions long kept as a form of paraffin blocks.

Ref.: Tsutsumi Y. Electron microscopic study using formalin-fixed, paraffin-embedded material, with special reference to observation of microbial organisms and endocrine granules. Acta Histochem Cytochem 2018; 51(2): 63-71. doi: 10.1267/ahc.18012

# Ultrastructural analysis using paraffin sections, particularly focused on infectious diseases

**Merits** using formalin-fixed, paraffin-embedded sections

1) We have a lot of target materials, and rare lesions can be analyzed.
2) The approach is suitable for the retrospective study.
3) The permeability of antibodies or probes is high.
4) The targeted approach can be achieved: highly accurate sampling from focal lesions can be done for EM analysis, after observing H&E-stained or specific-signalized paraffin-sections.
5) Particles of pathogens or endocrine granules can be observed as relatively stable fine structures.

**Demerits** using formalin-fixed, paraffin-embedded sections

1) Ultrastructural preservation is poor.

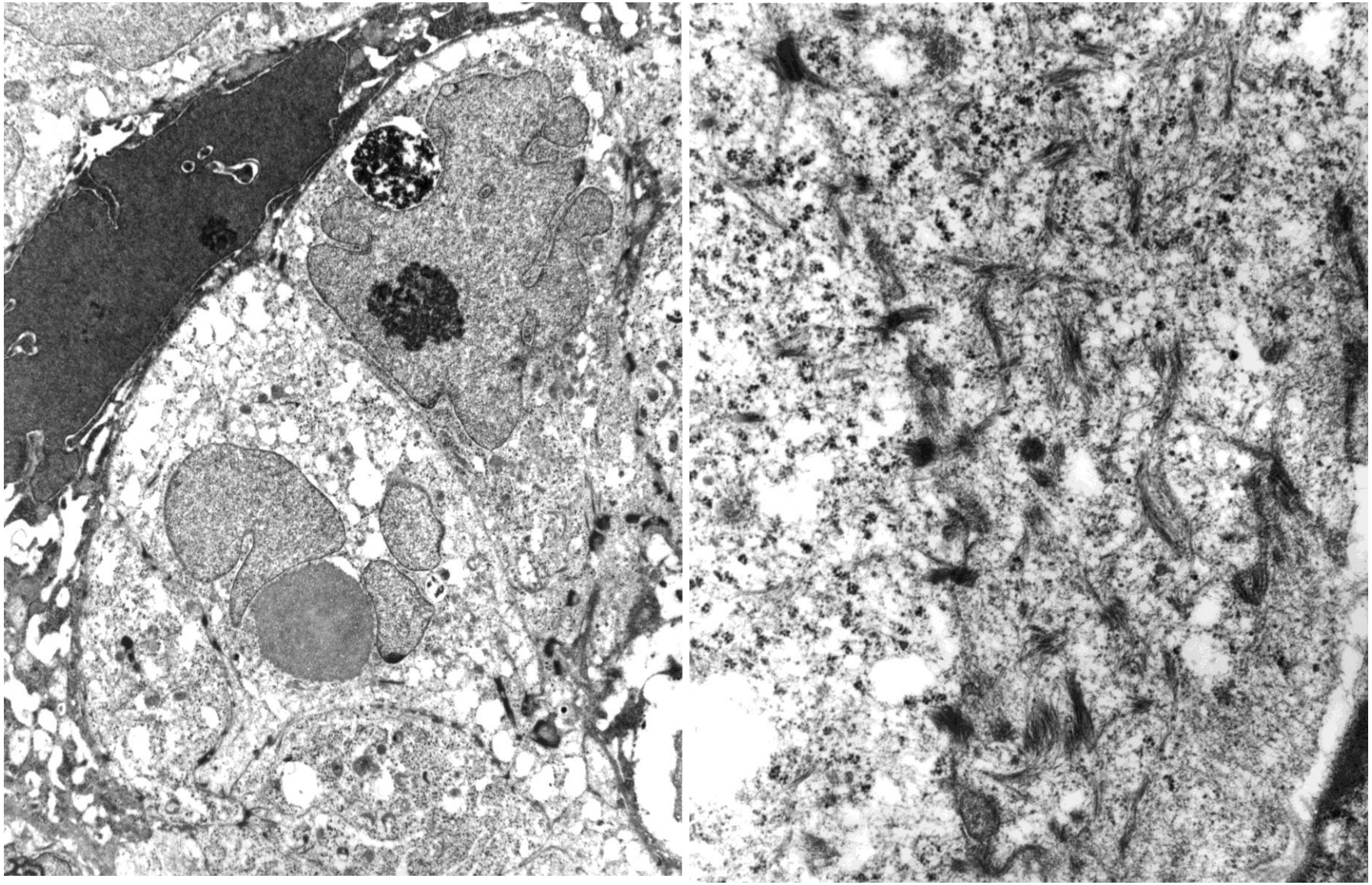

EM blocks were dug out of formalin-fixed, paraffin-embedded blocks as small cubes, and ultrathin sections were routinely prepared.  Poorly differentiated squamous cell carcinoma of the lung is shown here.  Morphological preservation of the nuclei and fine tonofilaments is excellent.

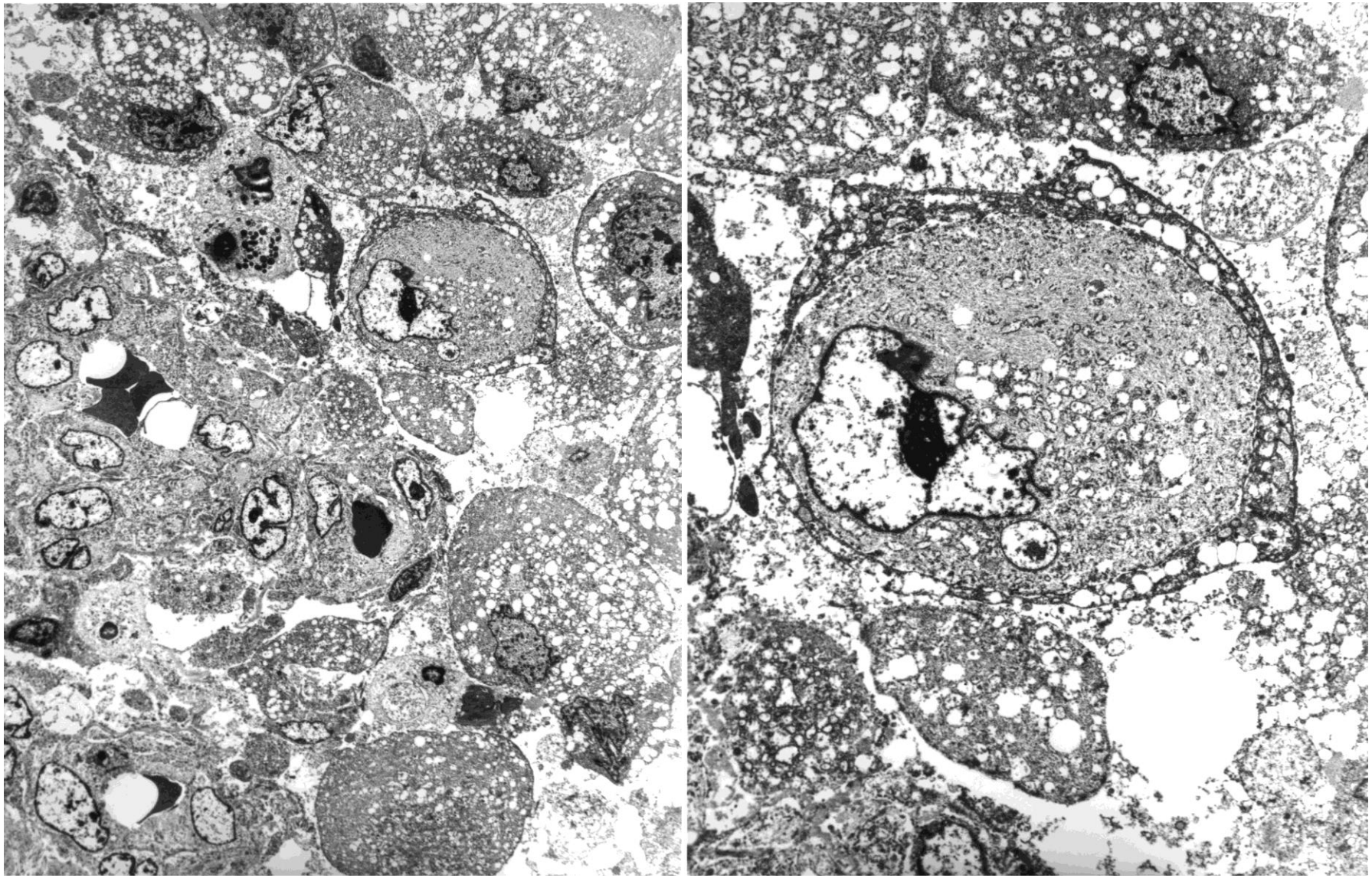

EM blocks were dug out of formalin-fixed, paraffin-embedded blocks as small cubes, and ultrathin sections were routinely prepared.  Anaplastic thyroid carcinoma is shown here.  Morphological preservation of the nuclei and cytoplasmic organelles and fine filaments is excellent.

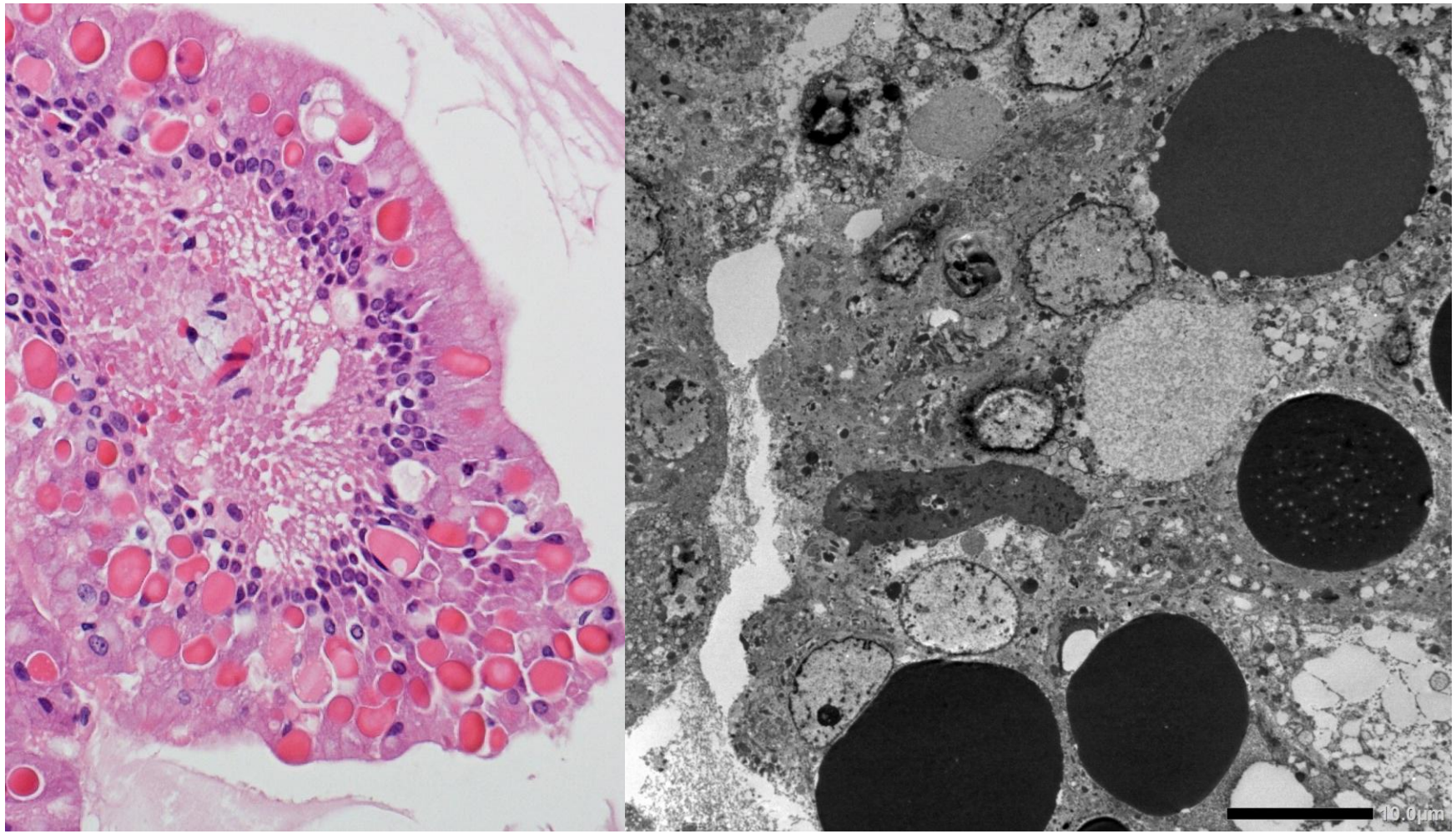


EM blocks were dug out of formalin-fixed, paraffin-embedded blocks as small cubes, and ultrathin sections were routinely prepared. Hyaline globules (thanatosomes) in pancreatic intraductal papillary mucinous neoplasm. HGs are round in shape and homogenously electron-dense, representing proteinaceous secretory materials. Fine morphological preservation is excellent. Ref. Tachibana M, et al. Pancreatic intraductal papillary mucinous neoplasm with hyaline globules (thanatosomes): report of two cases. Int Med Case Rep J 2021; 14: 393-399. doi: 10.2147/IMCRJ.S309766

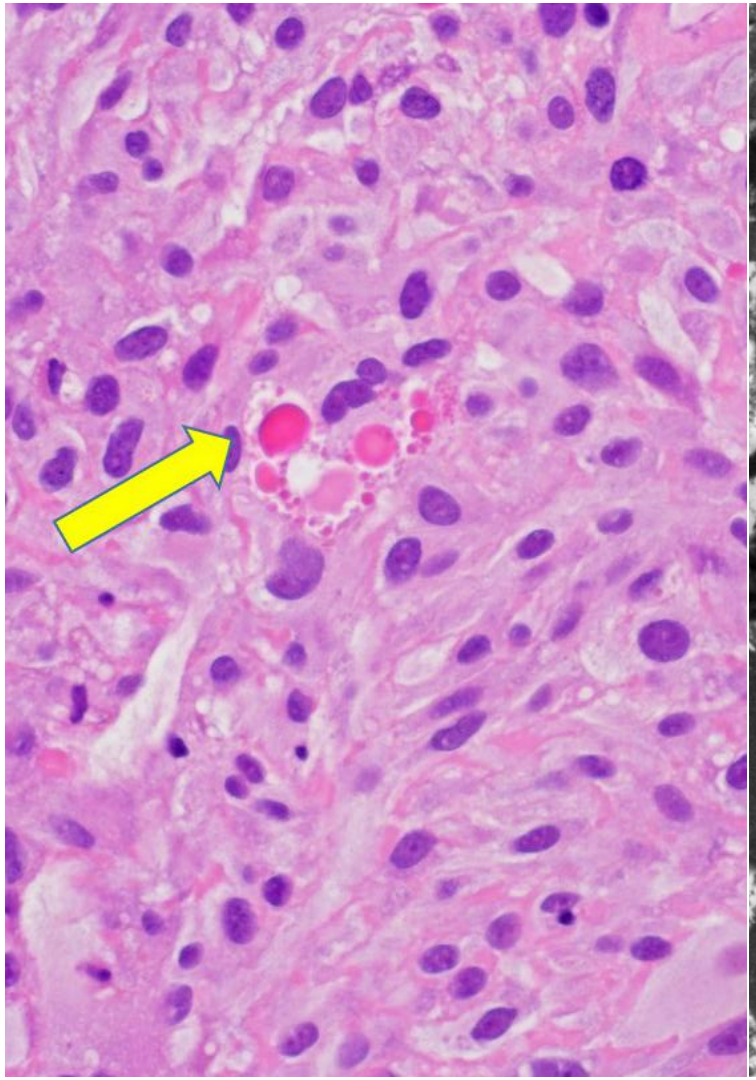

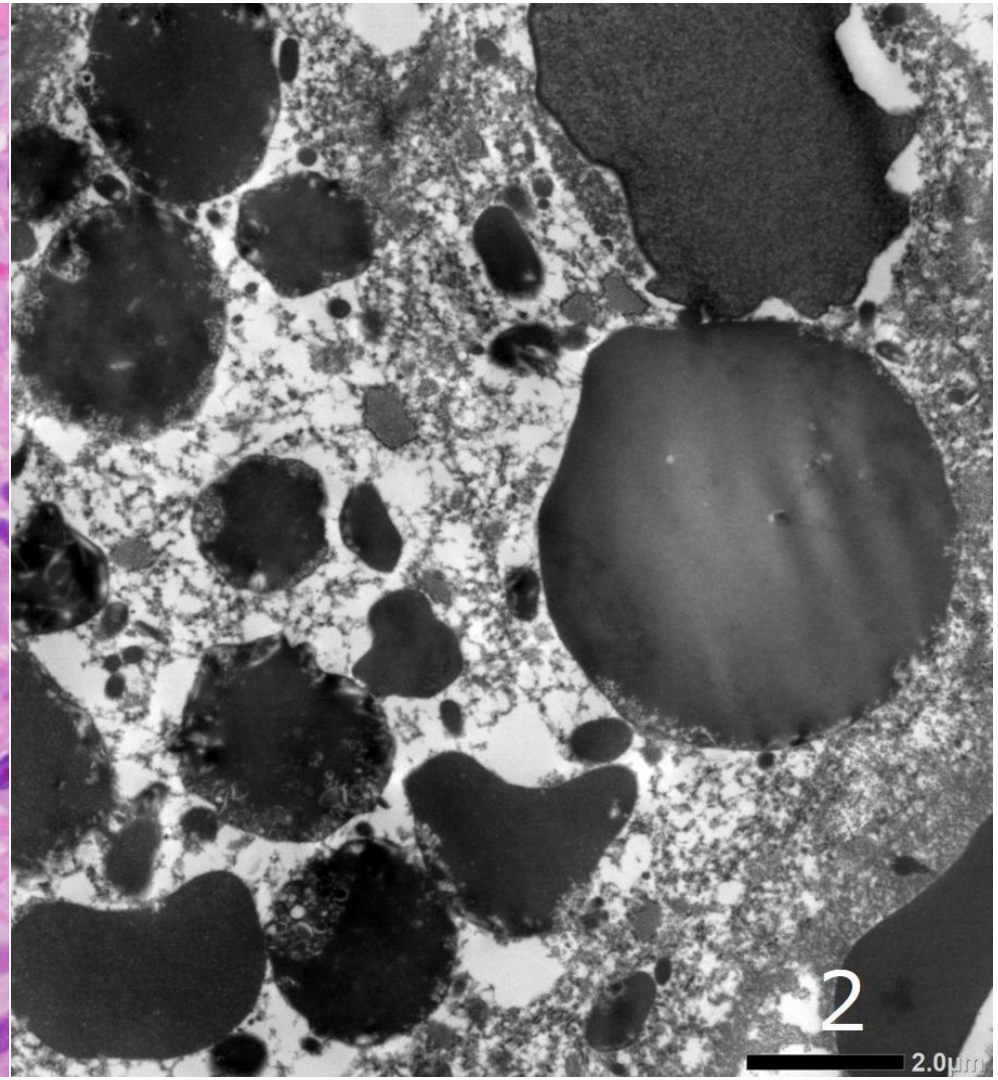


EM blocks were dug out of formalin-fixed, paraffin-embedded blocks as small cubes, and ultrathin sections were routinely prepared. Undifferentiated pleomorphic sarcoma of the left thigh accompanied hyaline globules (thanatosomes). HGs, immunoreactive for cleaved caspase-3, ultrastructurally show clusters of small-sized electron-dense globules with granular material in the globule matrix. They should be related to an apoptotic process of the tumor cells. Ref.: Tachibana M, et al. Undifferentiated pleomorphic sarcoma with hyaline globules (thanatosomes). Cureus 2021;13(6): e15789. doi: 10.7759/cureus.15789

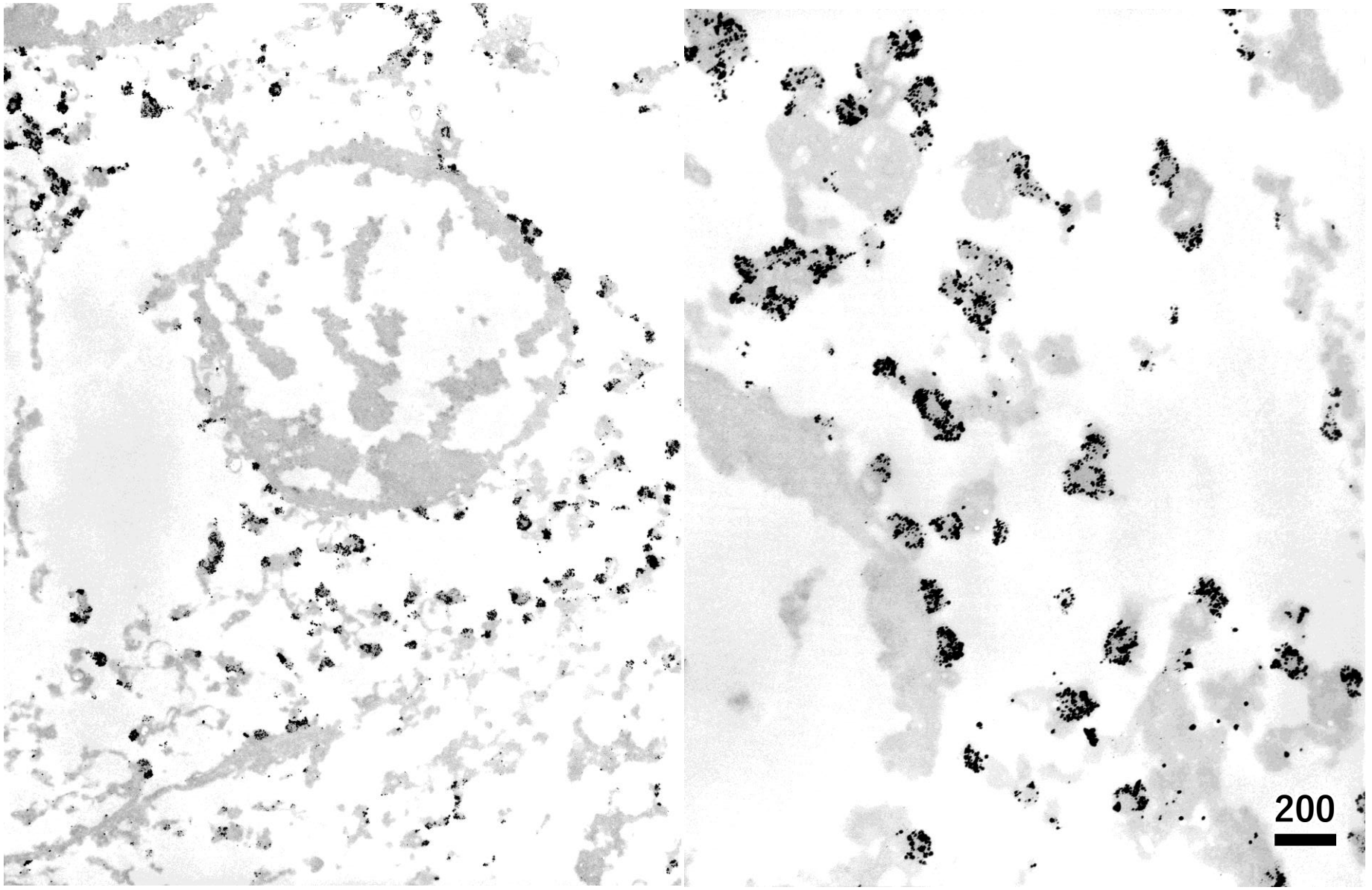


Grimelius-stained pulmonary tumorlet. Small argyrophilic neuroendocrine granules can be visualized. Argyrophilia is observed mainly at the peripheral portion of the granules.

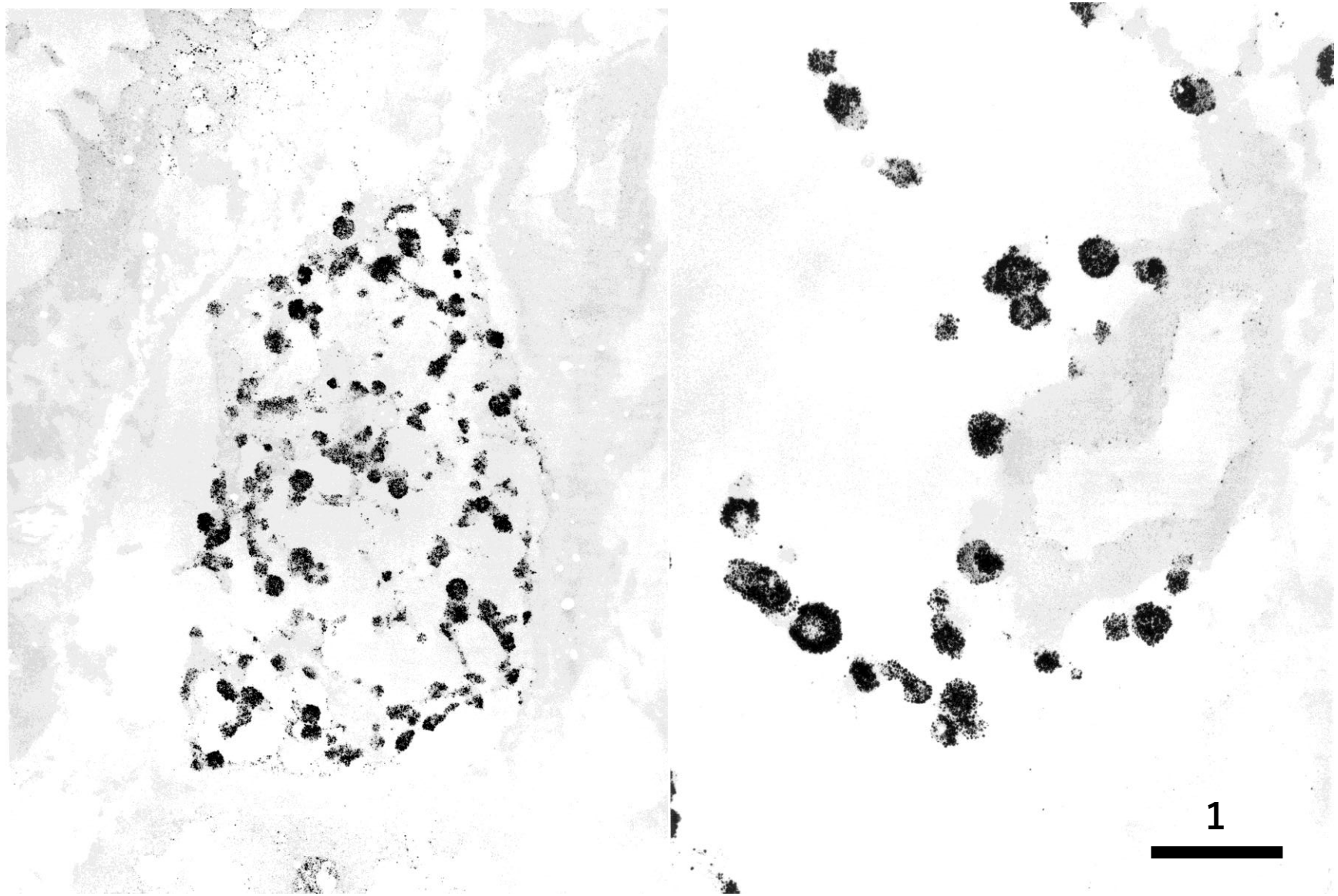


Ultrastructural features of Grimelius-positive argyrophilic neuroendocrine granules embedded in paraffin sections. Poorly differentiated scirrhous adenocarcinoma of the stomach with neuroendocrine components. Neuroendocrine granules of varying sizes are clustered in the cytoplasm of some cancer cells.

# Viral infections ultrastructurally proven in paraffin sections of the autopsy tissues of 10 y-o boy with acute lymphoblastic leukemia

The patient received HLA-mismatched CD34-positive stem cell transplantation for the treatment of ALL. Diarrhea started 1 week later, and bloody stool soon followed. Massive hemorrhage in the stool killed the patient in 3 months. No hematuria was recorded. At autopsy, graft versus host disease was confirmed. Intranuclear viral inclusions were seen in the small intestinal and urinary bladder mucosae.

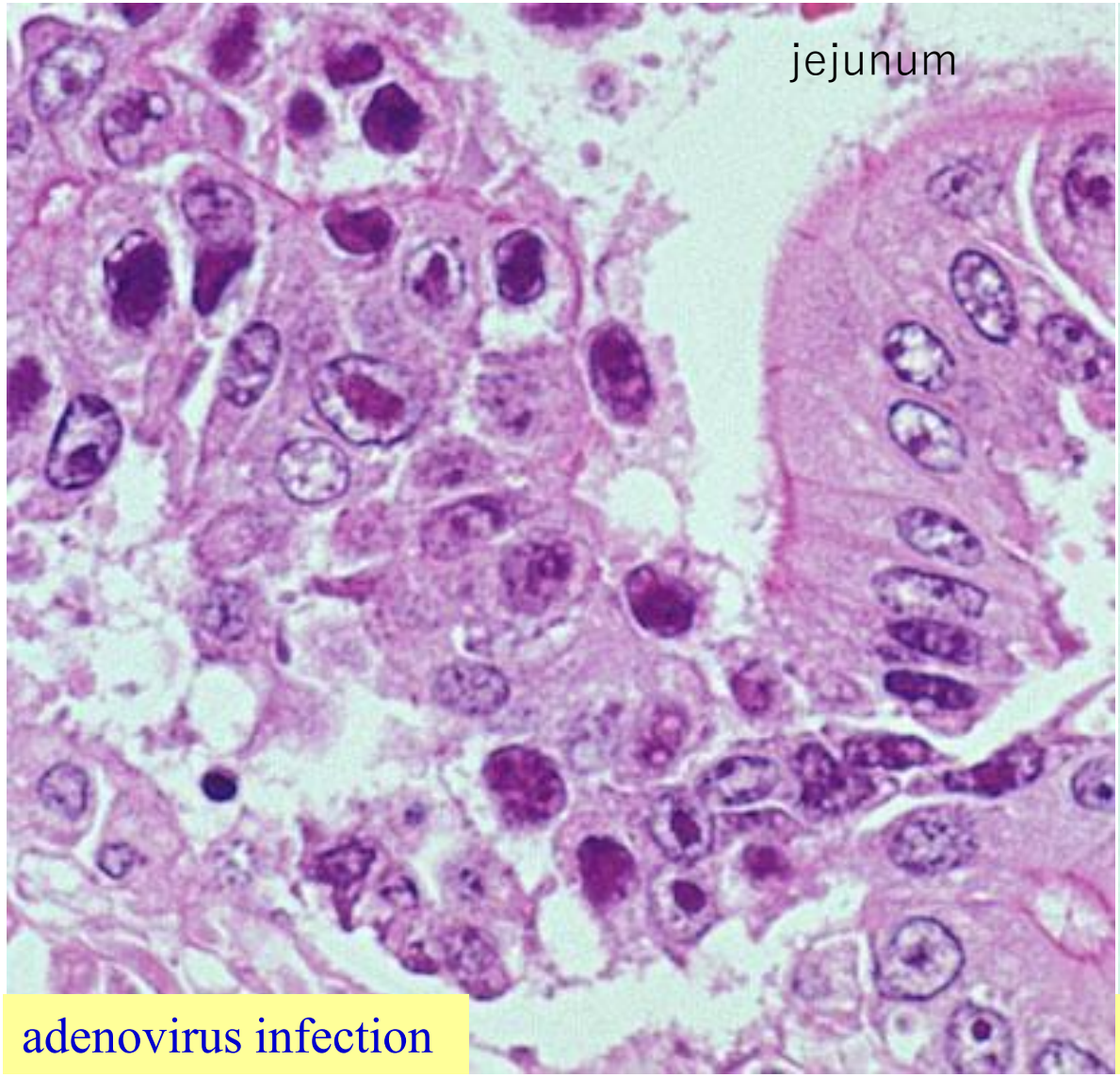


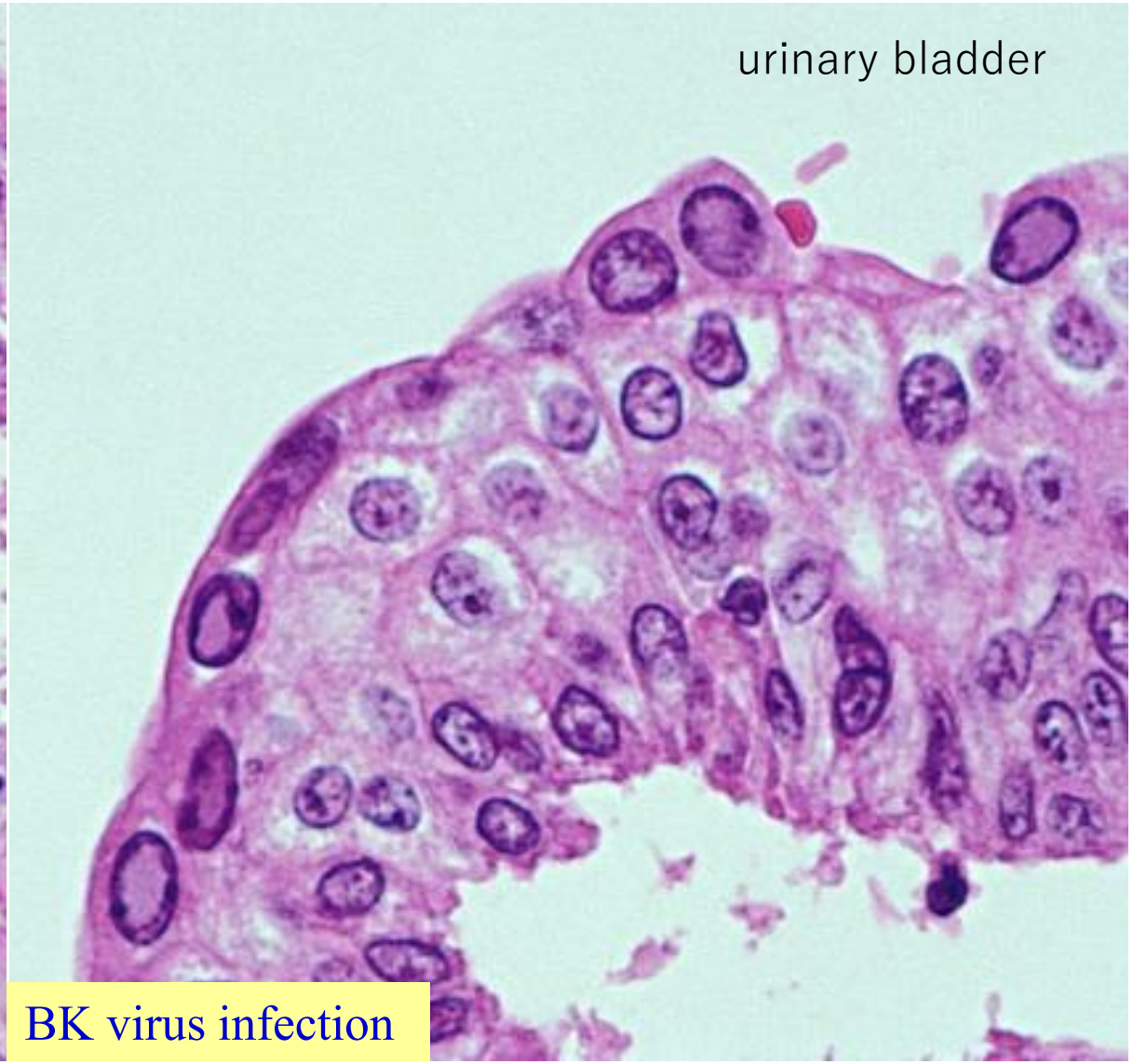


Columnar epithelial cells of the jejunal mucosa (left) and the umbrella cells of the urinary bladder mucosa (right) show intranuclear viral inclusions. The cells with the inclusion bodies in the respective paraffin sections were targeted for ultrastructural study.

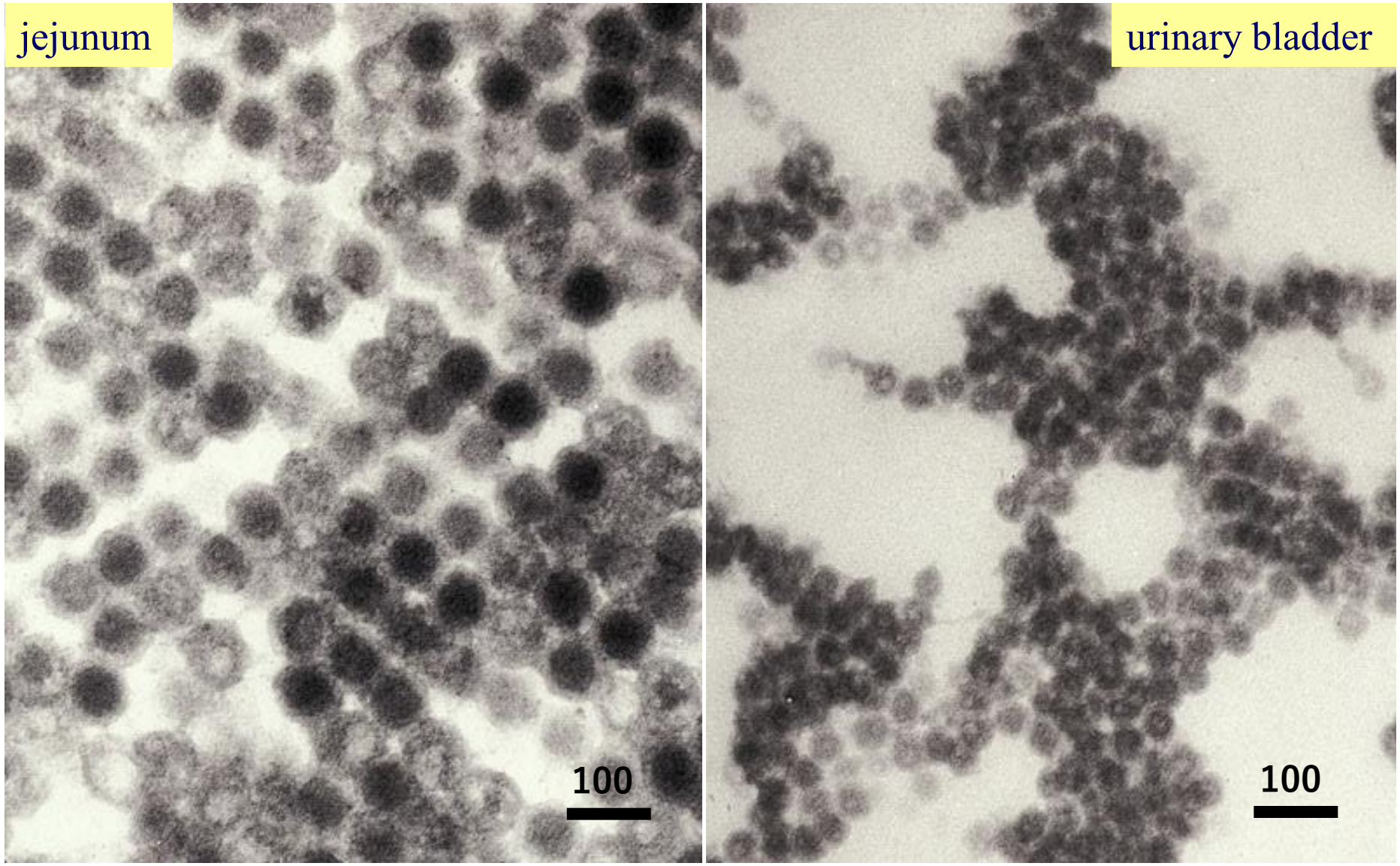


The viral particles in the nuclei of the jejunal mucosa (left) and urinary bladder mucosa (right) show features of adenovirus and polyoma virus, respectively. Adenoviral particles, 70 nm in size and regular hexagonal in shape, show a geometrical arrangement. The polyomavirus particles, 40 nm in size, are clustered haphazardly, being consistent with opportunistic BK virus infection.

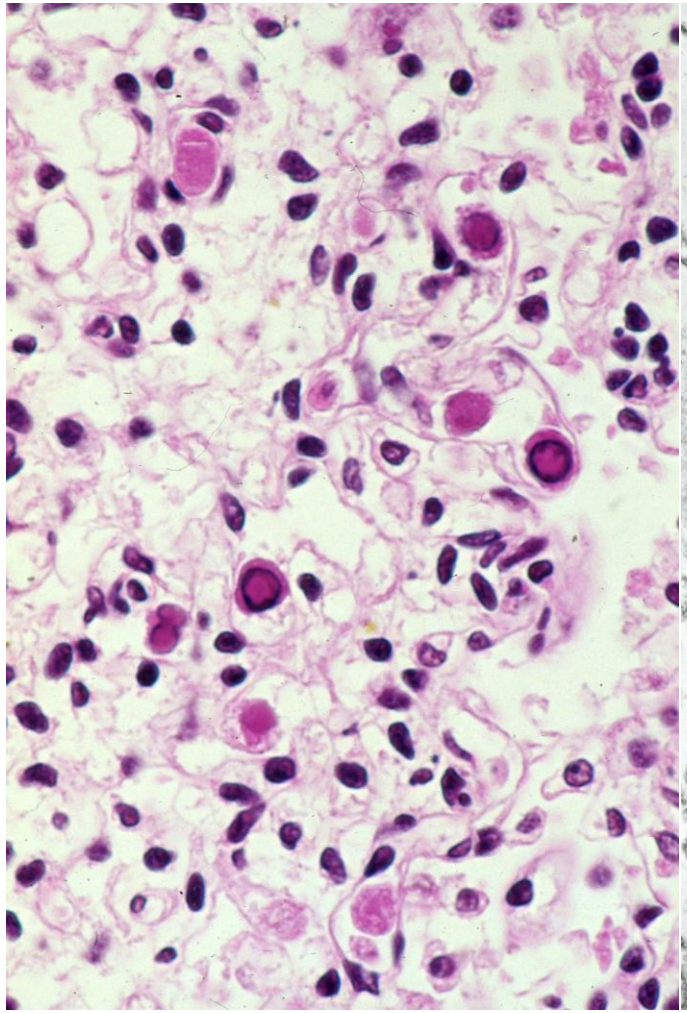


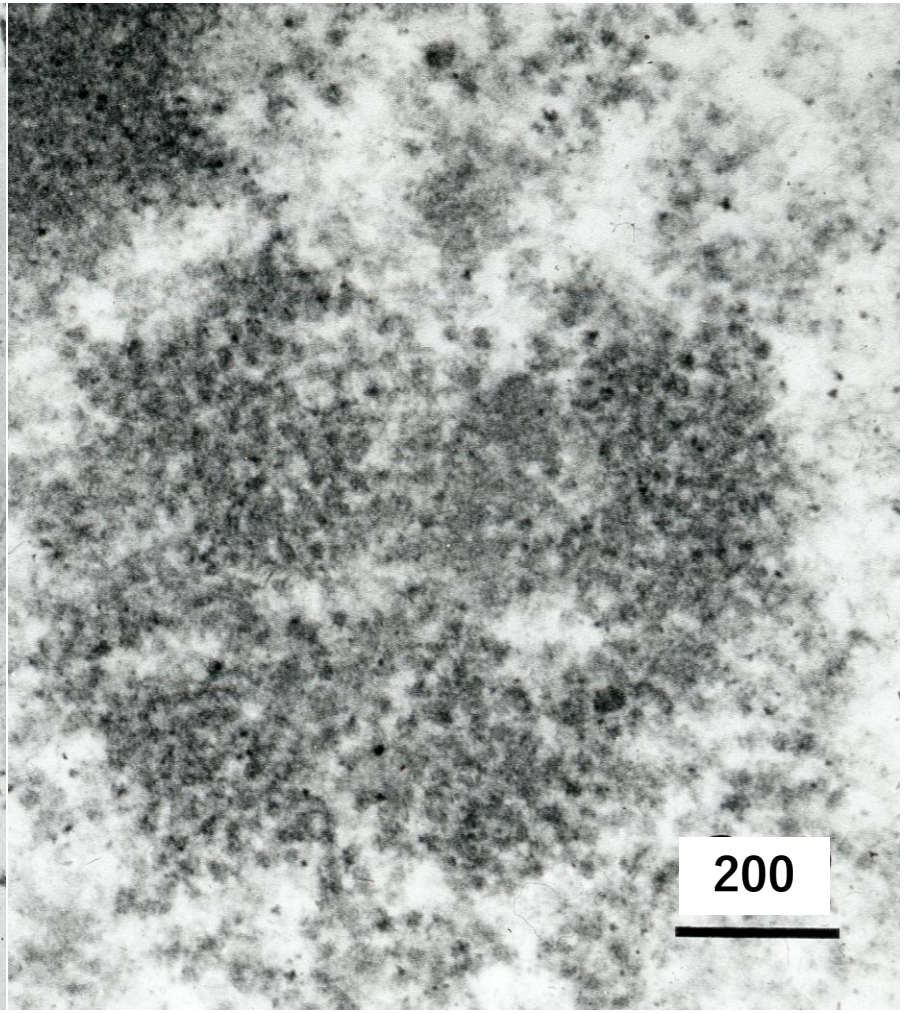


Autopsied lung in a macerated fetus (22 fetal weeks) with hydrops fetalis caused by parvovirus B19 infection. Erythroblasts (nucleated red cells) in the capillary vessel of the lung show eosinophilic intranuclear inclusions. Ultrastructural study was performed using formalin-fixed, paraffin-embedded sections to target the infected cells. The intranuclear inclusions contain 20 nm-sized small viral particles, being consistent with parvoviral infection.

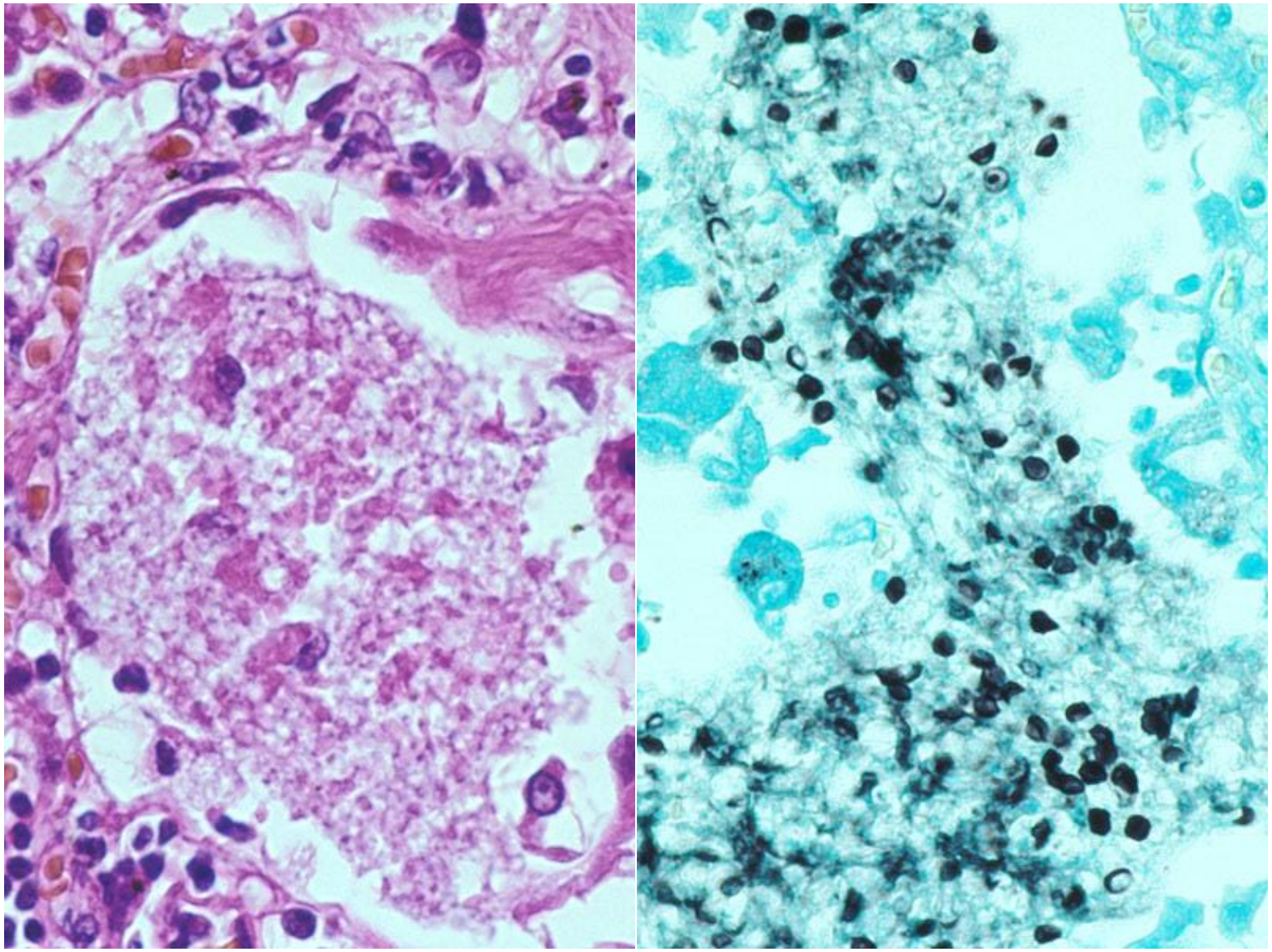

Autopsy lung with interstitial pneumonia caused by *Pneumocystis jirovecii* infection. Left; H&E, right: Grocott.  Grocott-reactive cysts are clustered in frothy exudates in the alveolar space.


Ultrastructural observation of Grocott-stained cysts of *Pneumocystis jirovecii* in formalin-fixed paraffin-embedded sections, The pre-embedding method was employed. The cell wall and dot-like structure of the pathogen are silver-impregnated.

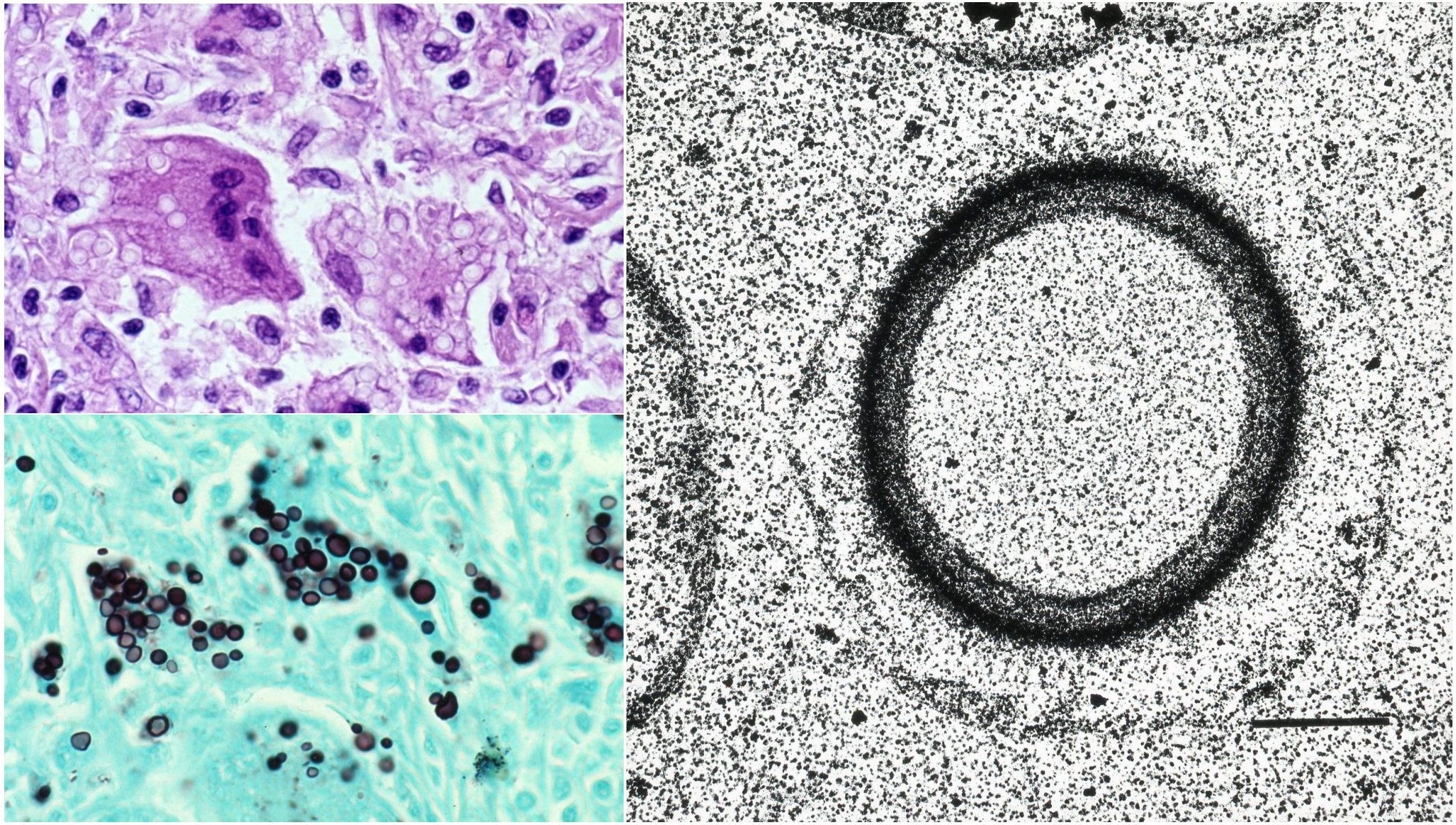

Cryptococcal granuloma of the lung.  Left top: H&E, left bottom: Grocott, right: ultrastructural features of Grocott-reactive yeasts in a macrophage.  Formalin-fixed, paraffin-embedded section stained with Grocott was ultrastructurally observed.  The cell wall is strongly silver-impregnated.

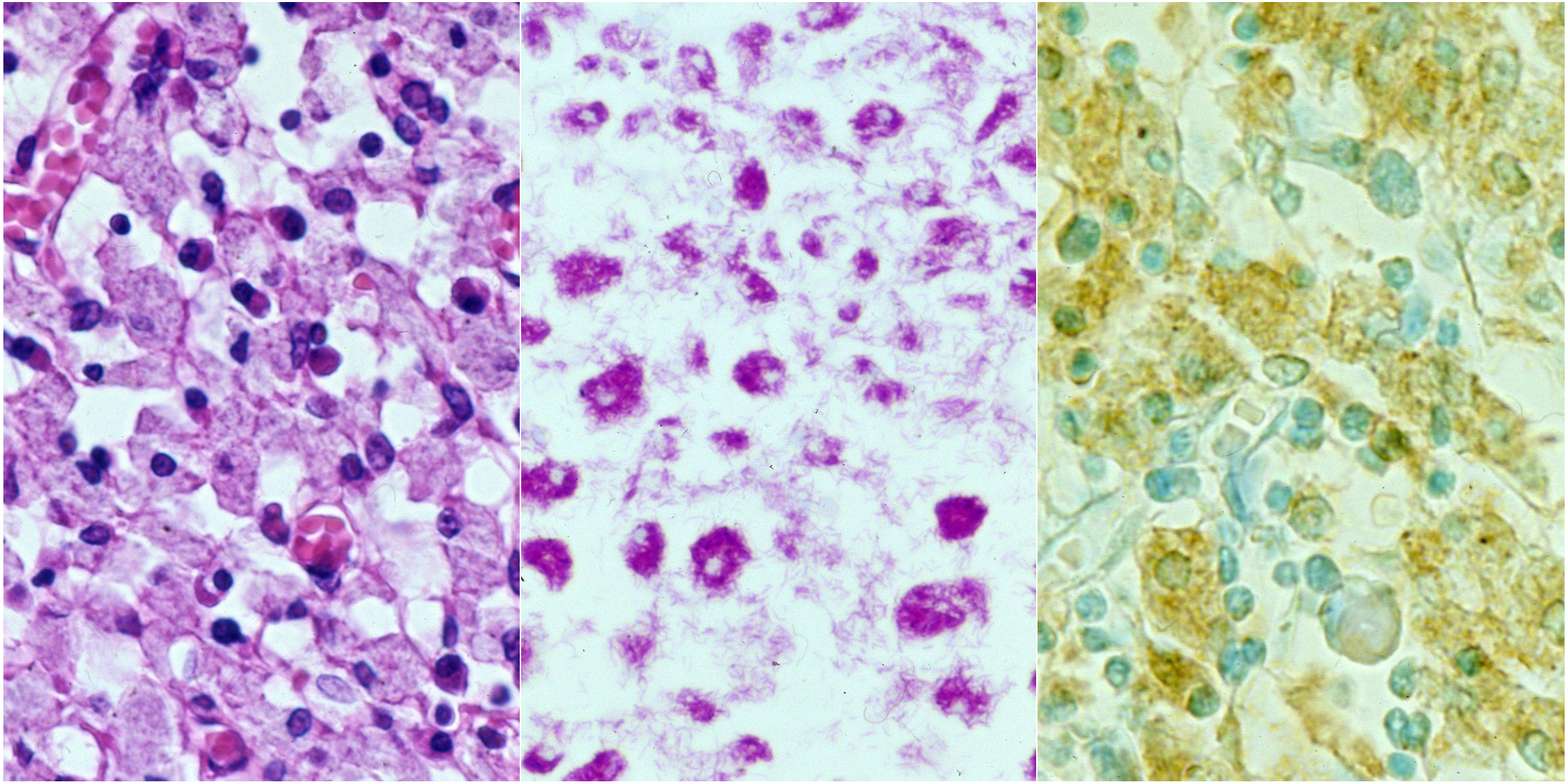

Opportunistic non-tuberculous Mycobacterium infection of the lung seen in a patient with AIDS. "Striated histiocytes" contain numerous acid-fast bacilli (*Mycobacterium aviun-intracellulare*: MAC) in the cytoplasm. Left: H&E, center: Ziehl-Neelsen, right: immunostaining for BCG antigens.

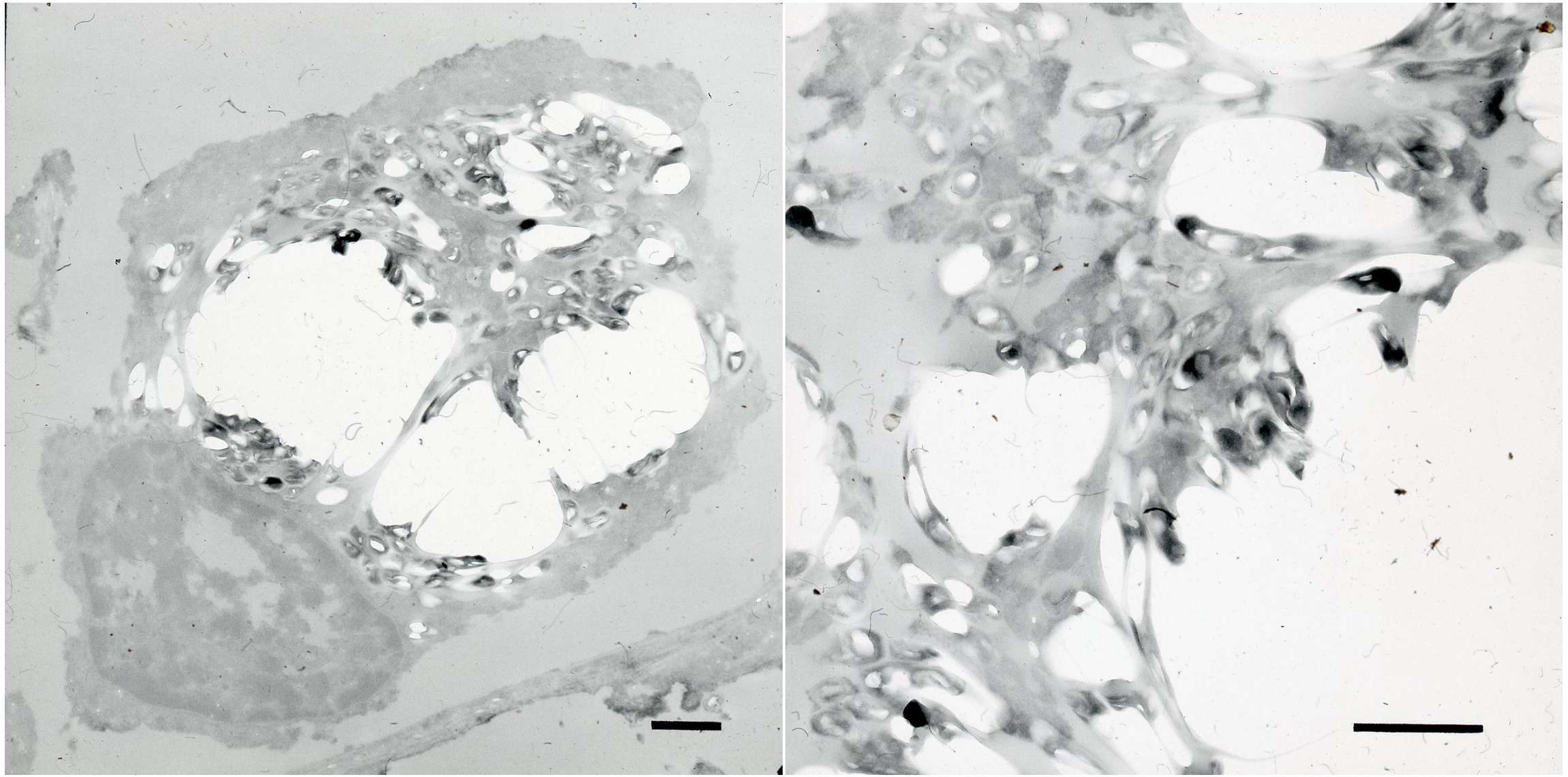

*Mycobacterium avium-intracellulare* (MAC) infection in AIDS. The "striated histiocyte" contains numerous BCG-immunoreactive rods in the cytoplasm. Pre-embedding immunoelectron microscopy for BCG antigens using formalin-fixed, paraffin-embedded section.

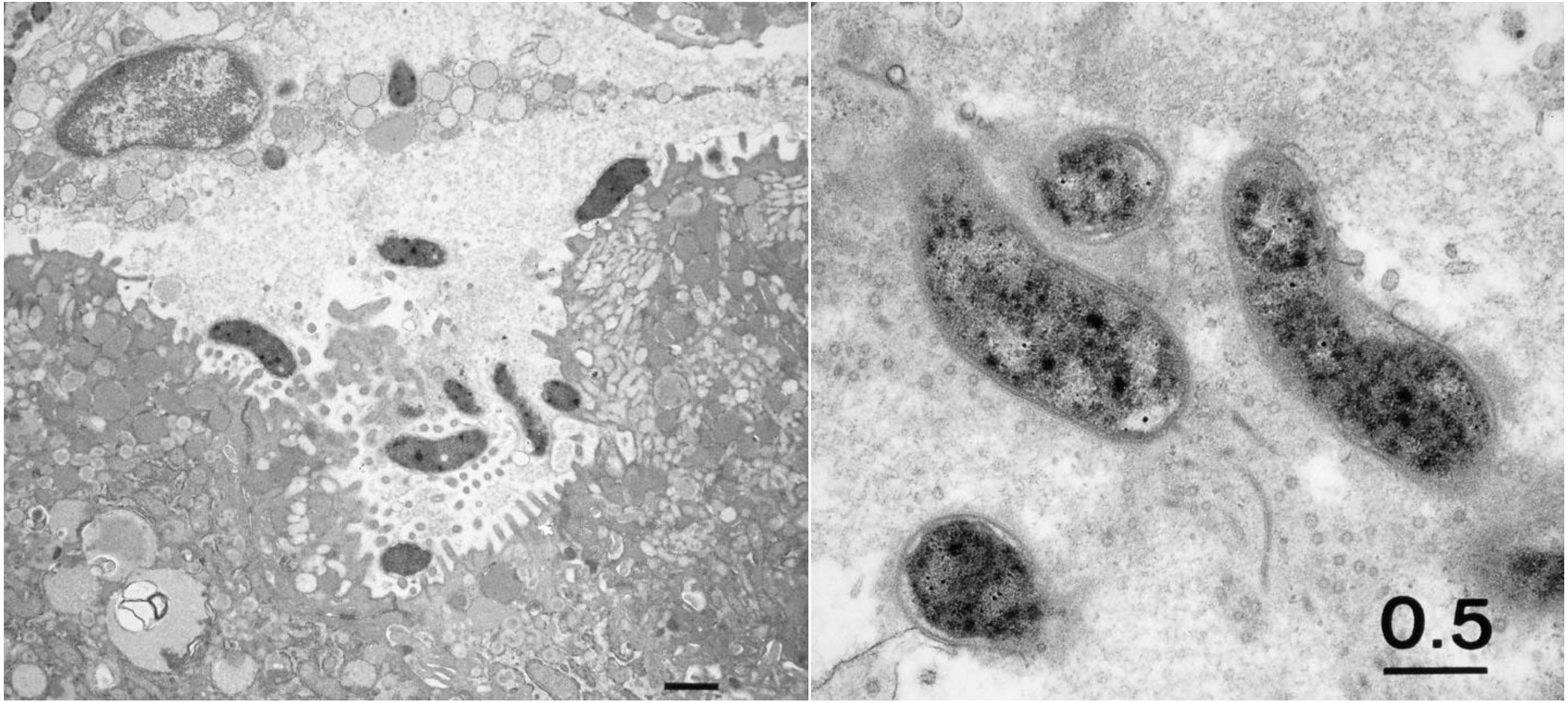


Ultrastructure of *Helicobacter pylori* infection on the gastric mucosa. The spiral bacteria with long flagellae infect on the gastric foveolar cells with microvilli on the apical plasma membrane. Conventional electron microscopy

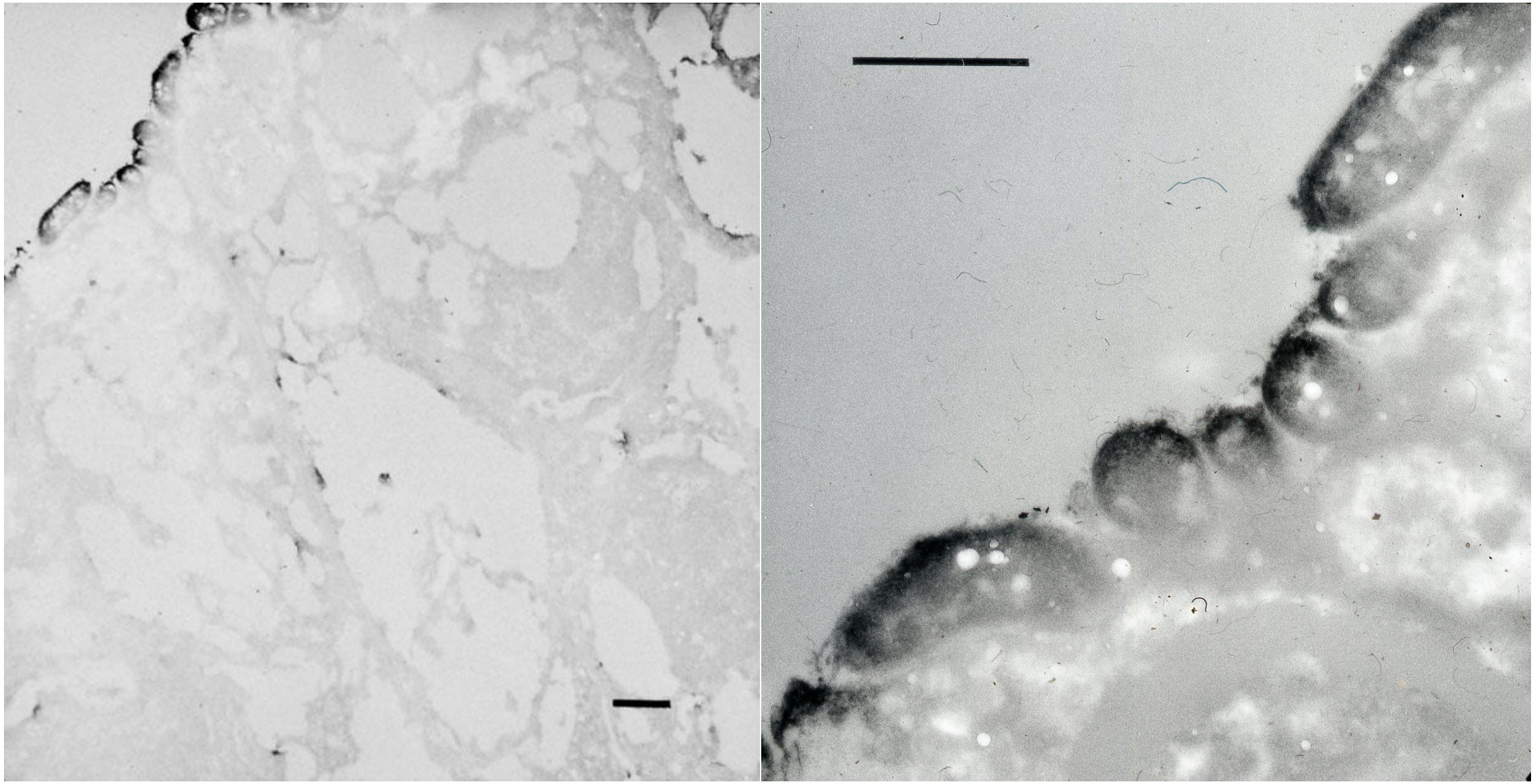

Immunoelectron microscopy of *Helicobacter pylori*-infected gastritis using formalin-fixed, paraffin-embedded gastric biopsy section. The *H. pylori* antigen-positive bacteria adhere onto the apical surface of the gastric foveolar cell.

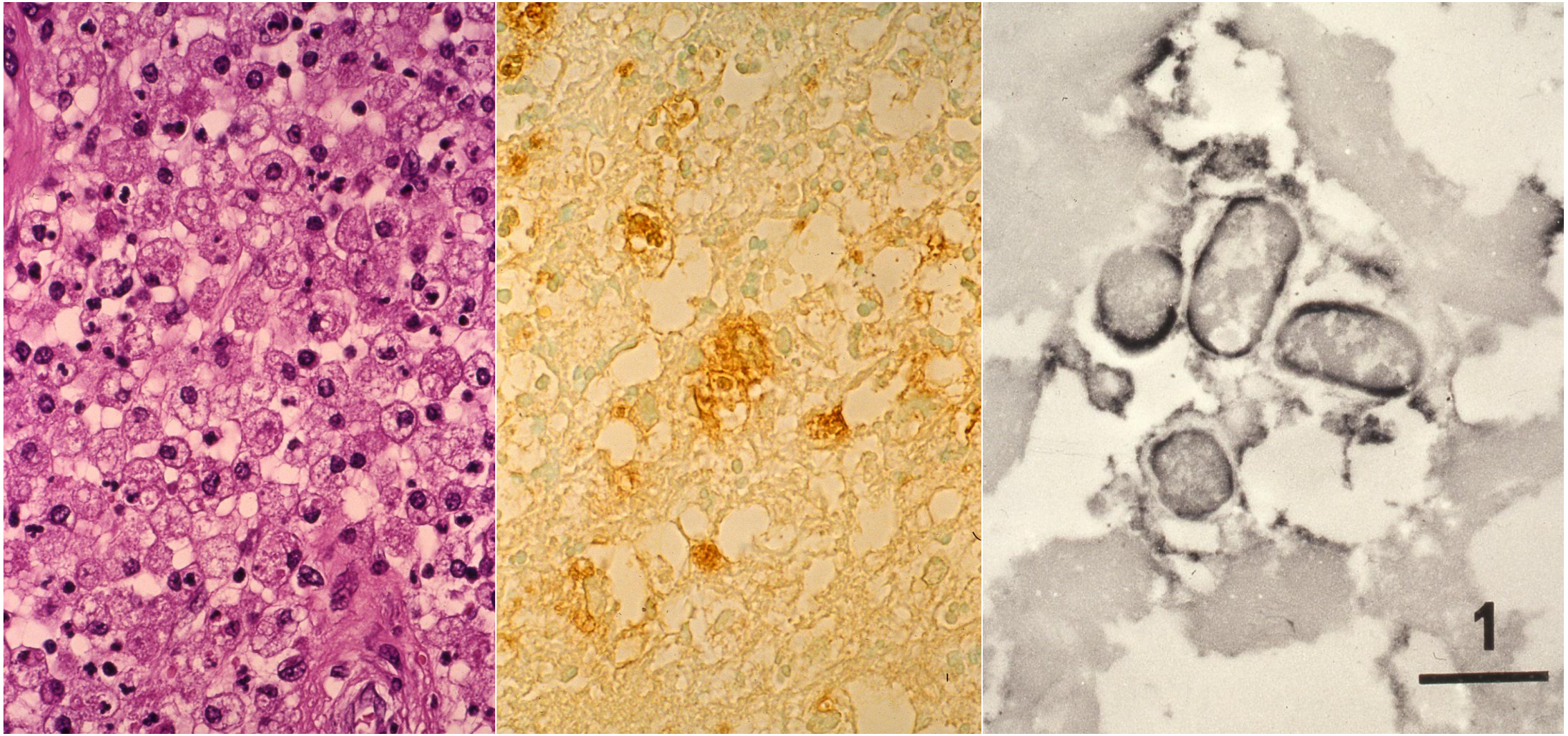


*E. coli*-induced xanthogranulomatous epididymitis. Left: H&E, center: immunostaining for *E. coli* antigens, right: pre-embedding immunoelectron microscopy for E. coli antigens using formalin-fixed, paraffin-embedded section. The cell wall of the rods phagocytized by a macrophage shows immunoreactivity. **Ref.**: Ref.: Hori S, Tsutsumi Y. Histological differentiation between chlamydial and bacterial epididymitis: nondestructive and proliferative versus destructive and abscess forming. Immunohistochemical and clinicopathological findings. Hum Pathol 1995; 26(4): 402-407. doi: 10.1016/0046-8177(95)90141-8

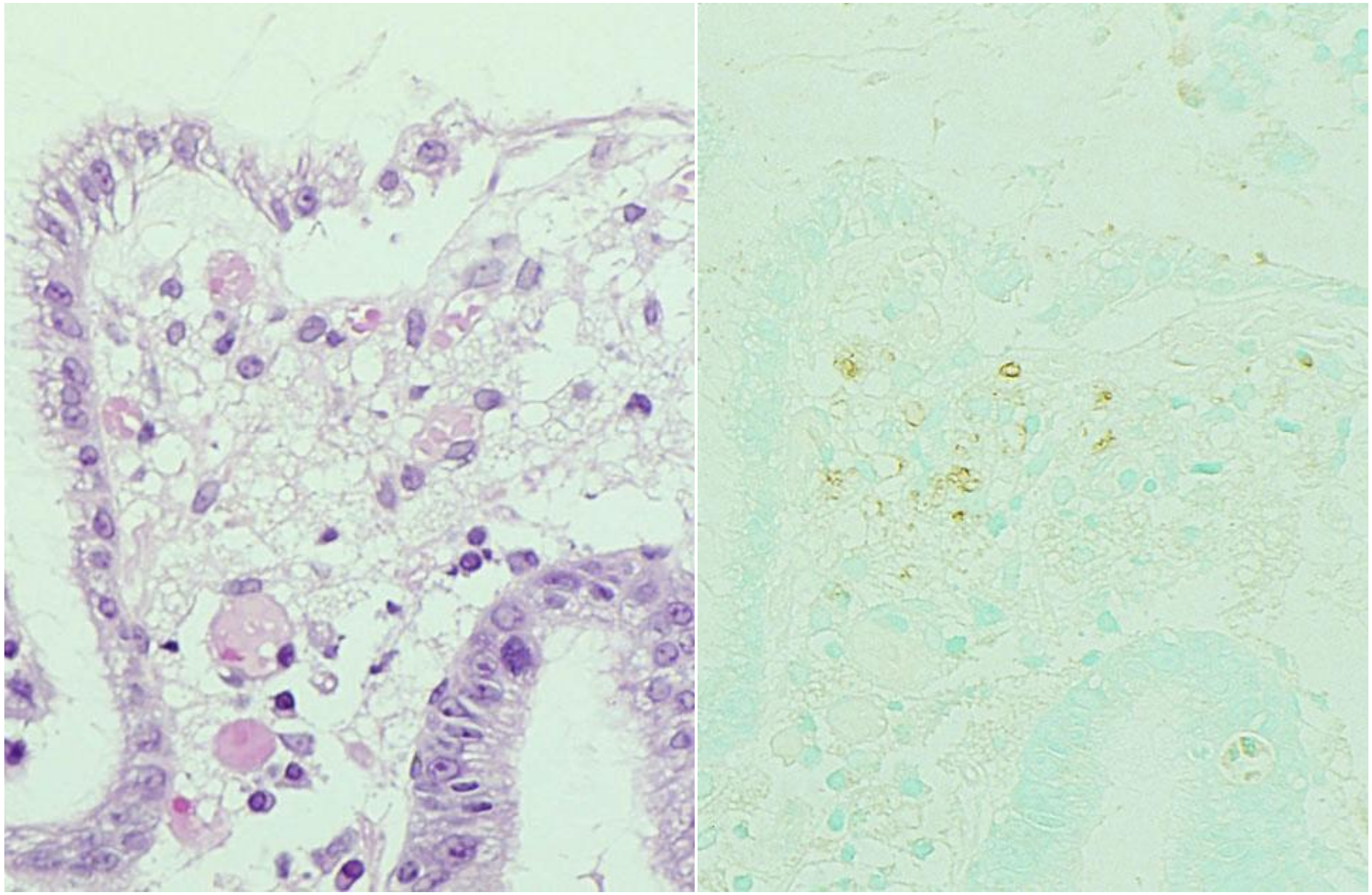

**Gastric xanthoma**. Left: H&E, right: immunostaining for *Helicobacter pylori* antigens. Most gastric xanthoma is associated with *H. pylori* infection, and the foamy macrophages phagocytize the bacteria.

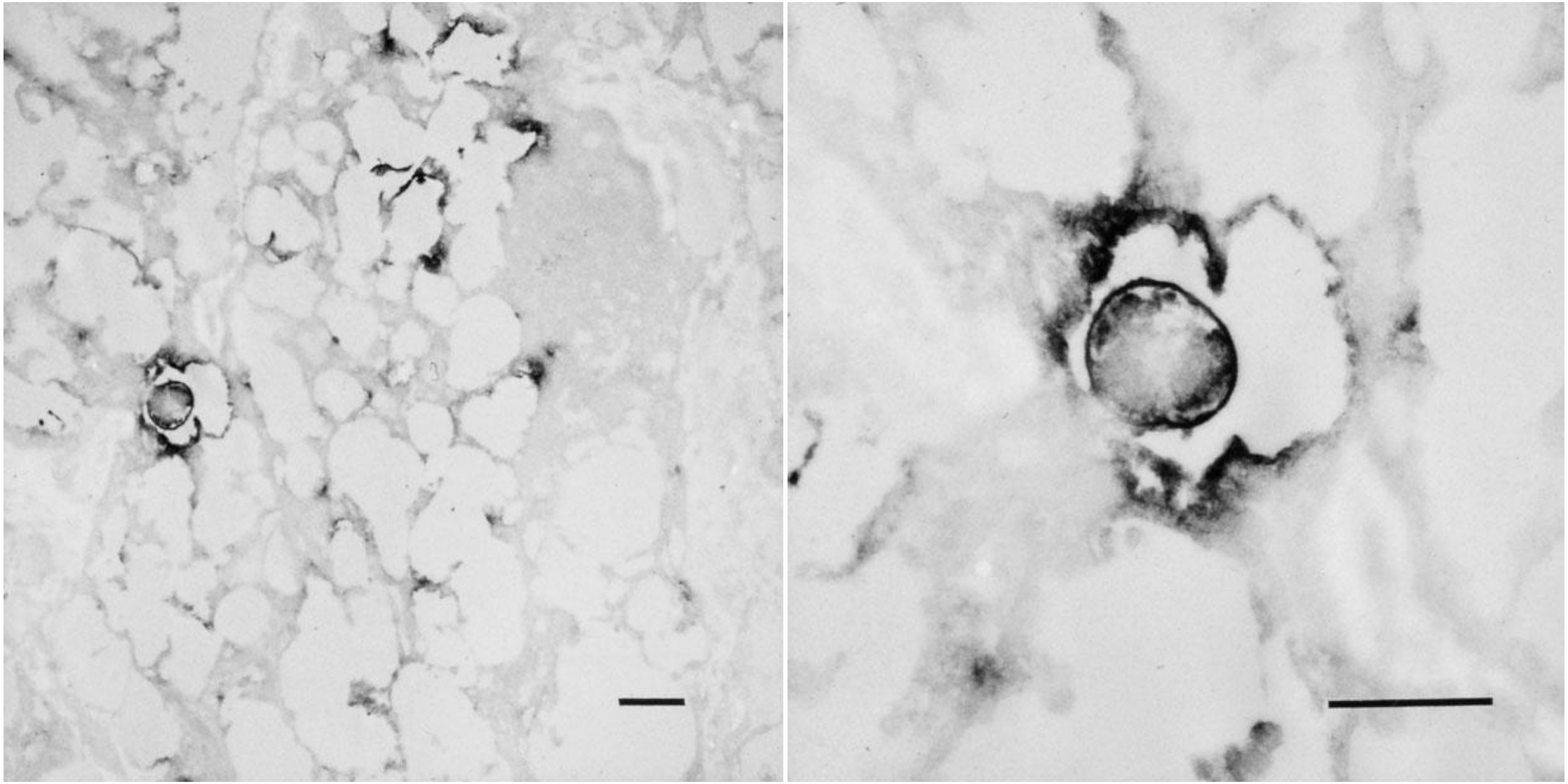

**Gastric xanthoma**: immunoelectron microscopy for *Helicobacter pylori* antigens using formalin-fixed, paraffin-embedded sections. The cytoplasm of the xanthoma cells (foamy macrophages) contain bacteria with positive signals of *H. pylori* antigens. The lipid component is derived from bacterial components. Ref.: Hori S, Tsutsumi Y. *Helicobacter pylori* infection in gastric xanthomas: immunohistochemical analysis of 145 lesions. Pathol Int 1996; 46(8): 589-593. doi: 10.1111/j.1440-1827.1996.tb03658.x

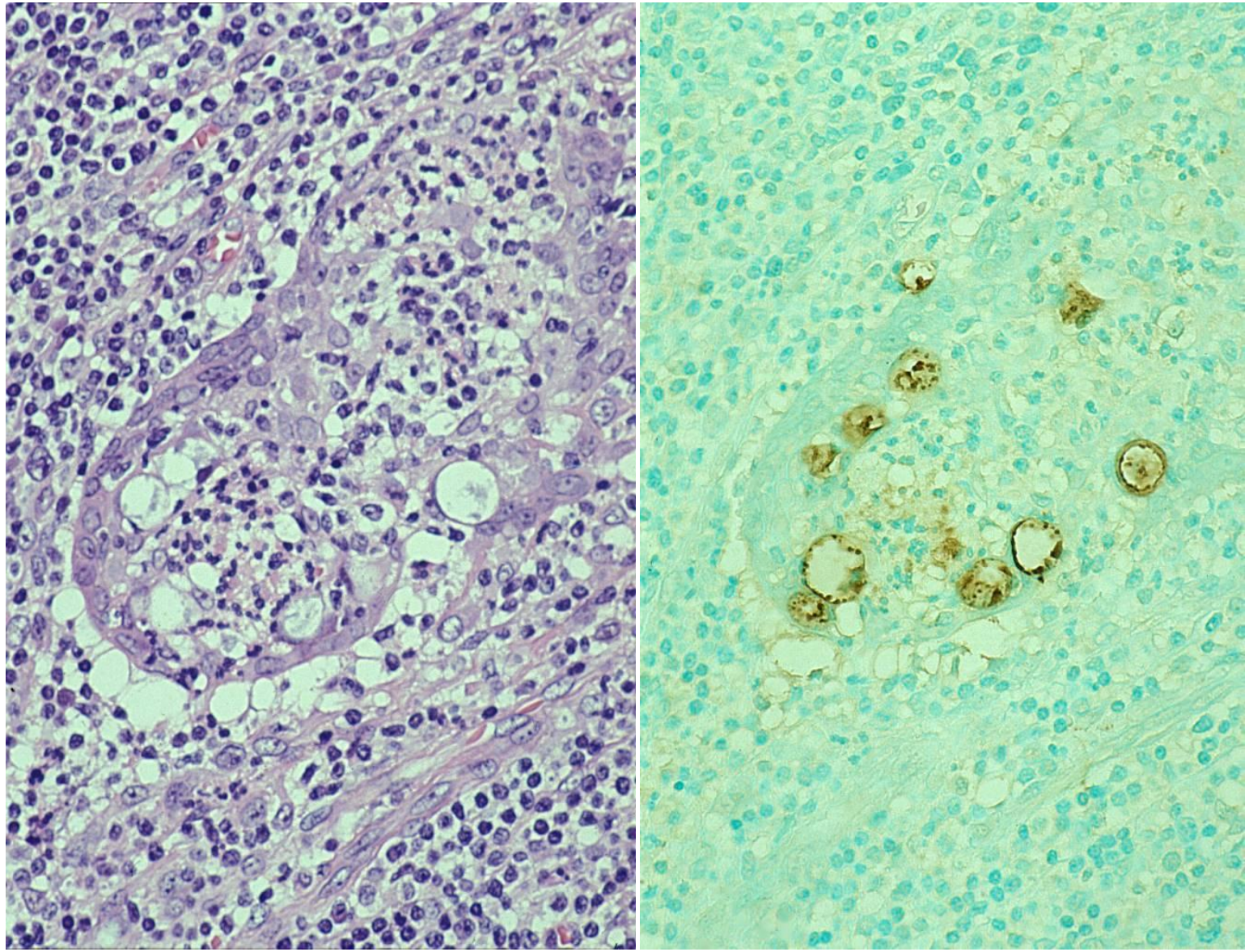

**Chlamydial epididymitis**. Surgical specimen with a clinical diagnosis of epididymal tumor. Left: H&E, right: immunostaining for *Chlamydia trachomatis* antigen. Cytoplasmic inclusion bodies are filled with chlamydial particles.

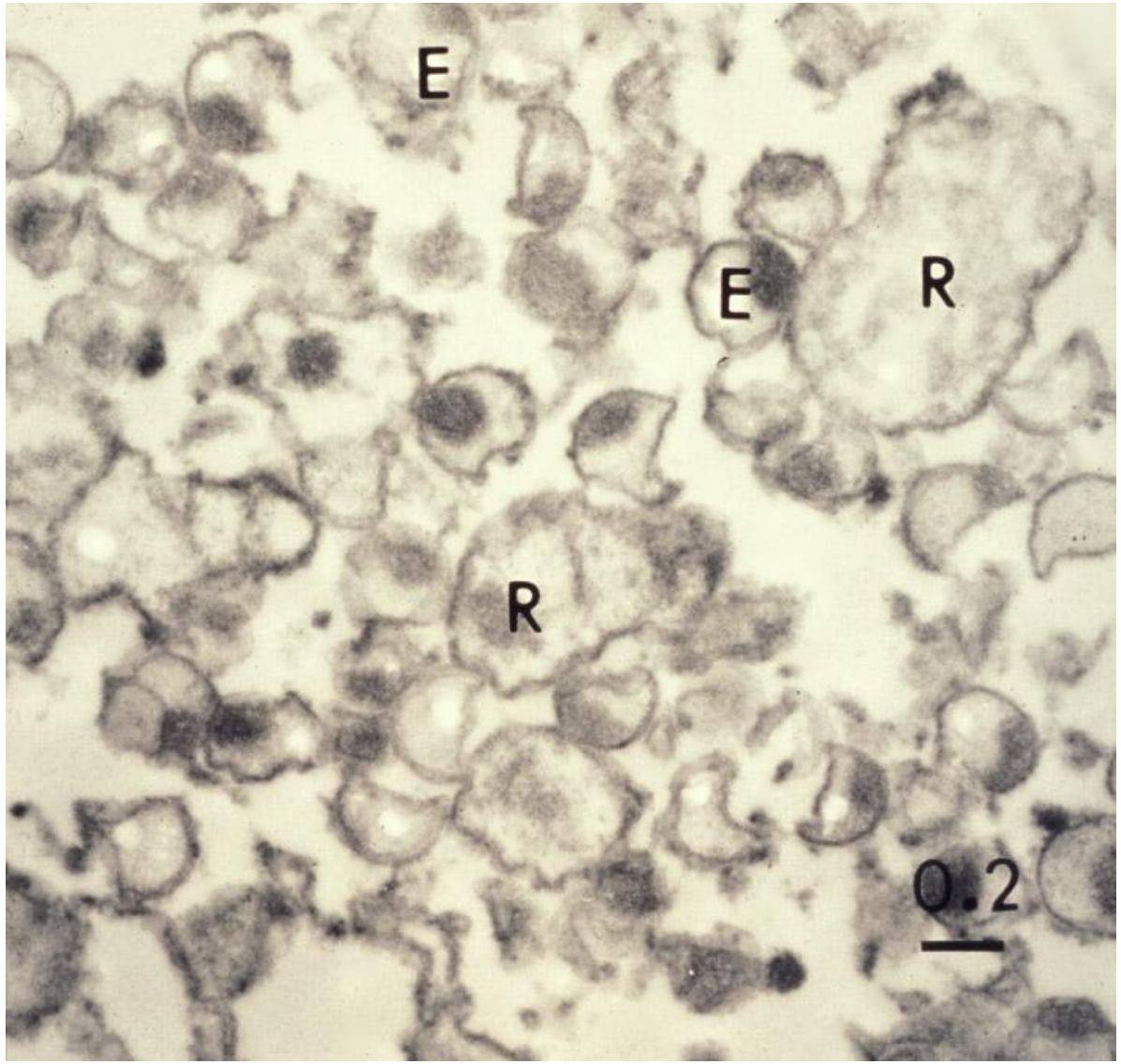


**E**: small-sized elementary bodies (infectious particles),
**R**: large-sized reticular bodies (proliferative particles)

Immunoelectron microscopy for chlamydial antigen in formalin-fixed, paraffin-embedded section of the surgical specimen of **chlamydial epididymitis**. The cell wall positivity is evident. **Ref.**: Hori S, Tsutsumi Y. Histological differentiation between chlamydial and bacterial epididymitis: nondestructive and proliferative versus destructive and abscess forming. Immunohistochemical and clinicopathological findings. Hum Pathol 1995; 26(4): 402-407. doi: 10.1016/0046-8177(95)90141-8

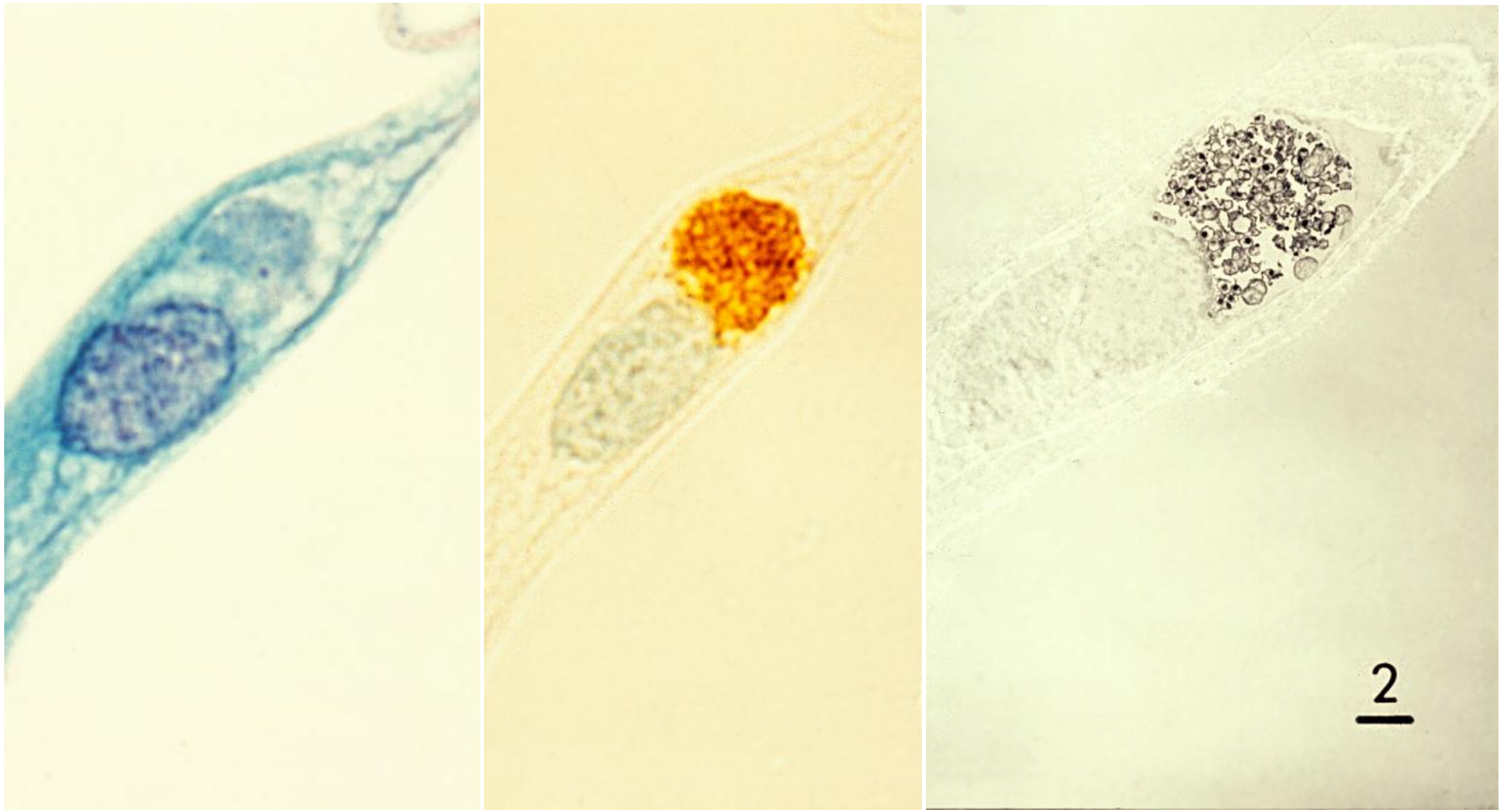


Immunoelectron microscopy using routine cytology material. Chlamydial cervicitis in cervical pap smear: nevular inclusion body in a metaplastic cell. Left: Pap, center: immunostaining for *Chlamydia trachomatis* antigen, right: pre-embedding immunoelectron microscopy using the Pap-smeared (ethanol-fixed) specimen. **Ref.**: Hori S, et al. Immunoelectron microscopic detection of chlamydial antigens in Papanicolaou-stained routine vaginal smears. Acta Cytol 1995; 39(4): 835-837. PMID: 7631568

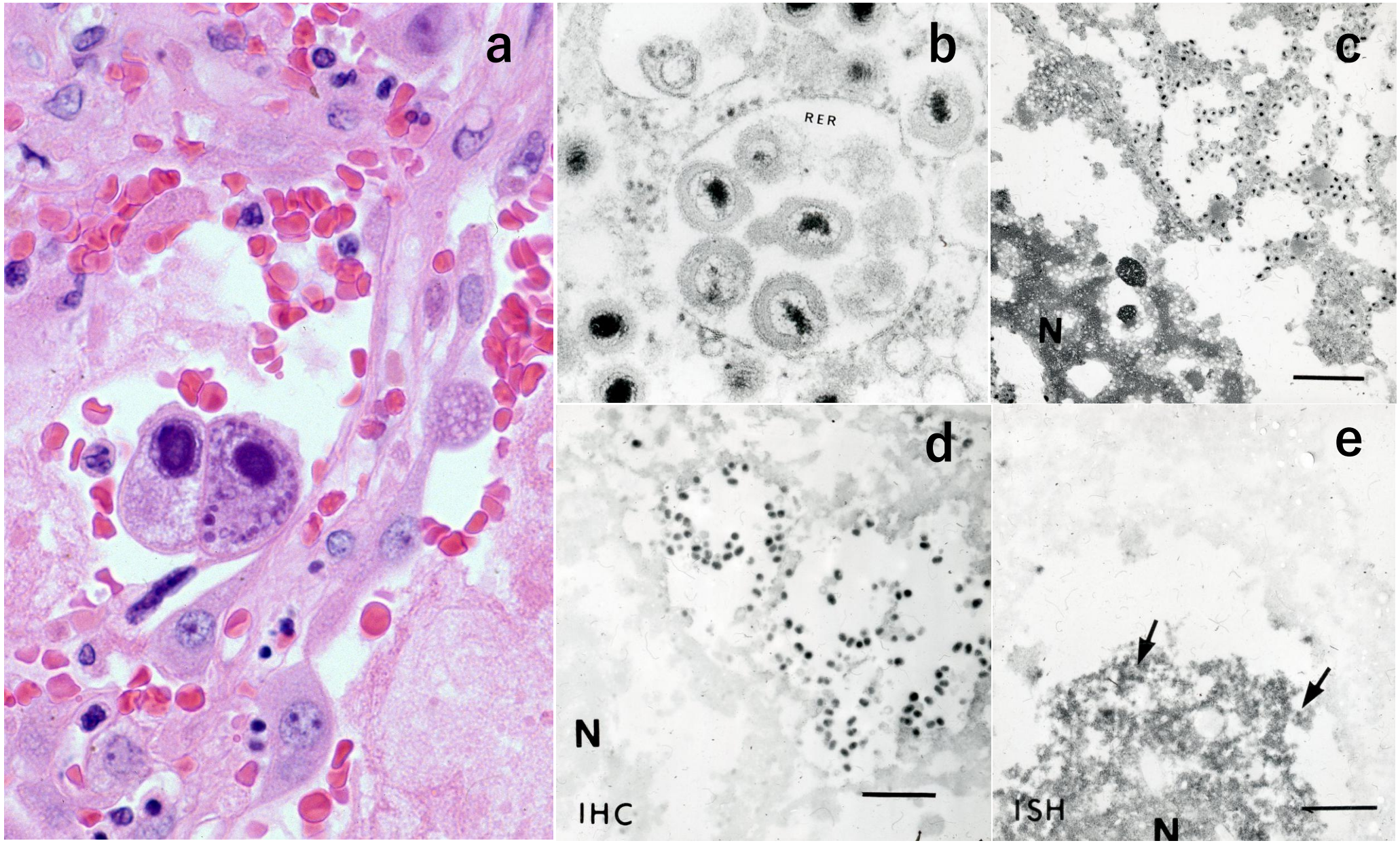


Cytomegalic inclusion disease of the lung. a: H&E, b: conventional EM study, c: EM study using a paraffin section, d: immunoelectron microscopy for CMV antigen, e: *in situ* hybridization for CMV genome at the EM level. RER: rough endoplasmic reticulum, N: nucleus

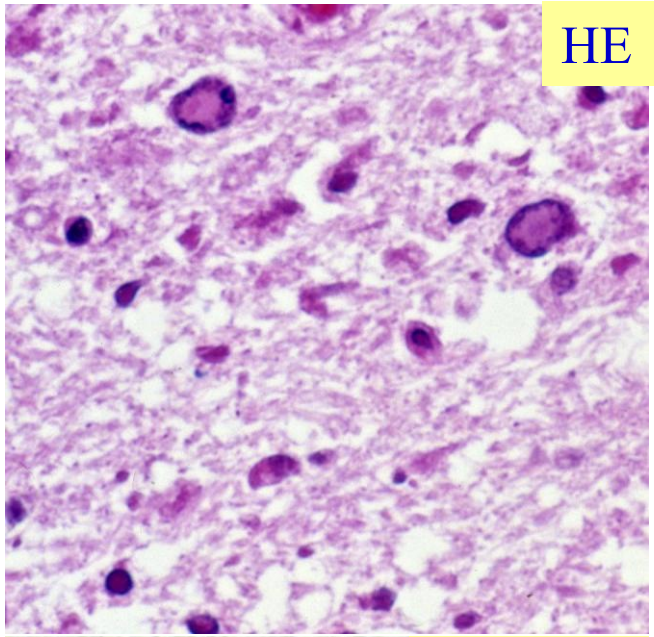


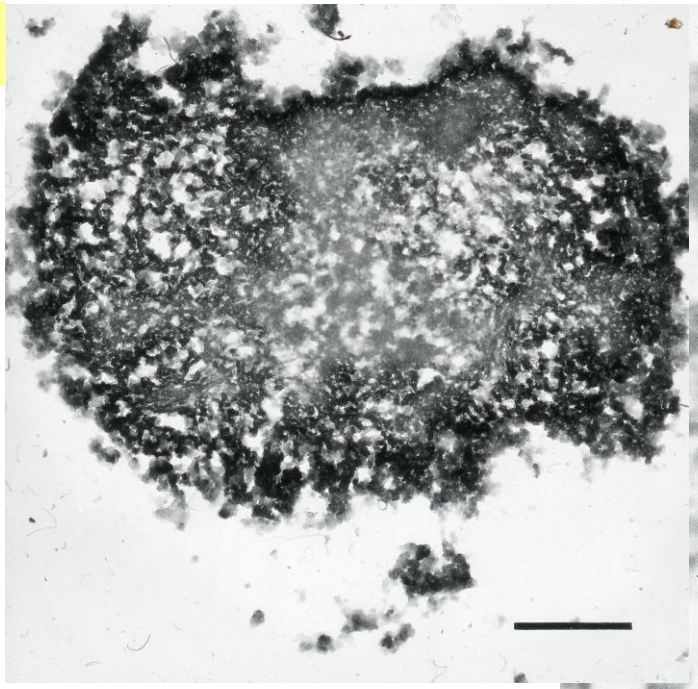

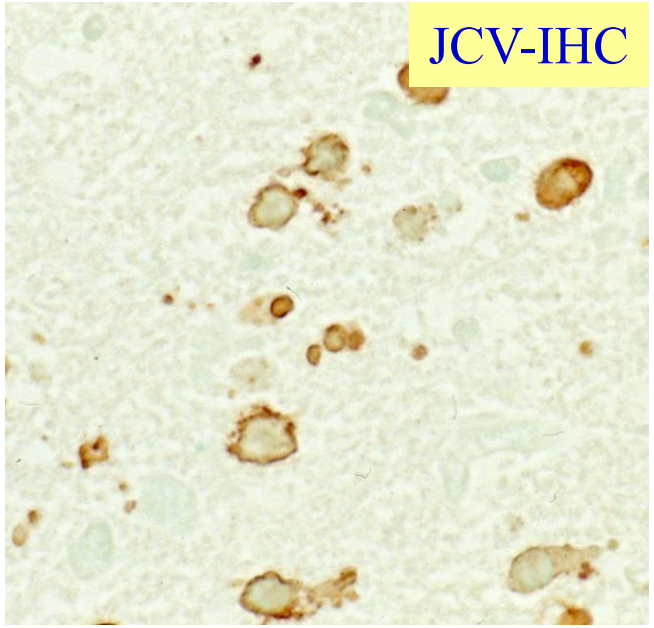


Progressive multifocal leukoencephal-opathy (JC virus infection)

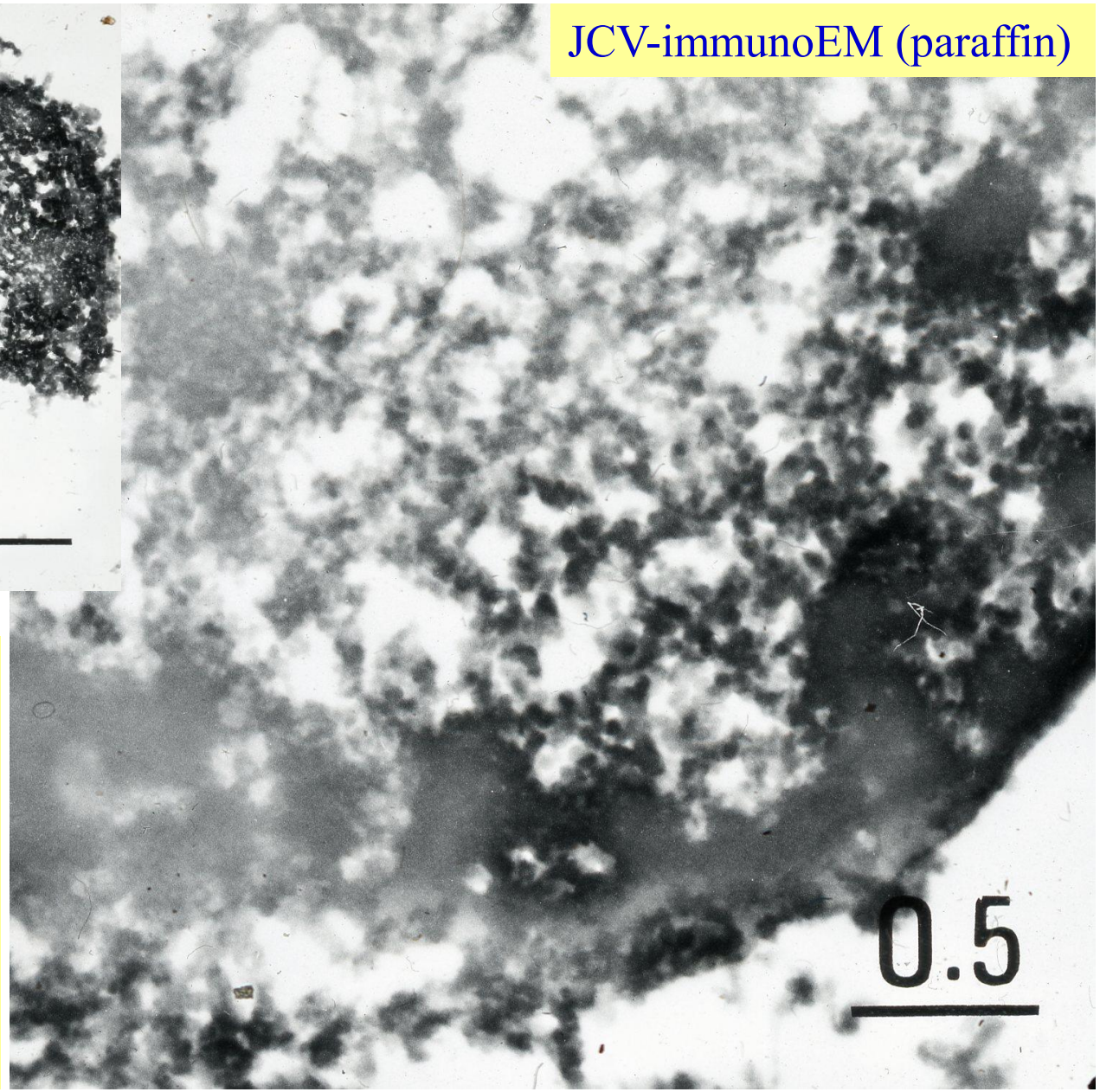


JCV particles are observed in the nuclei of glial cells in formalin-fixed, paraffin-embedded sections.

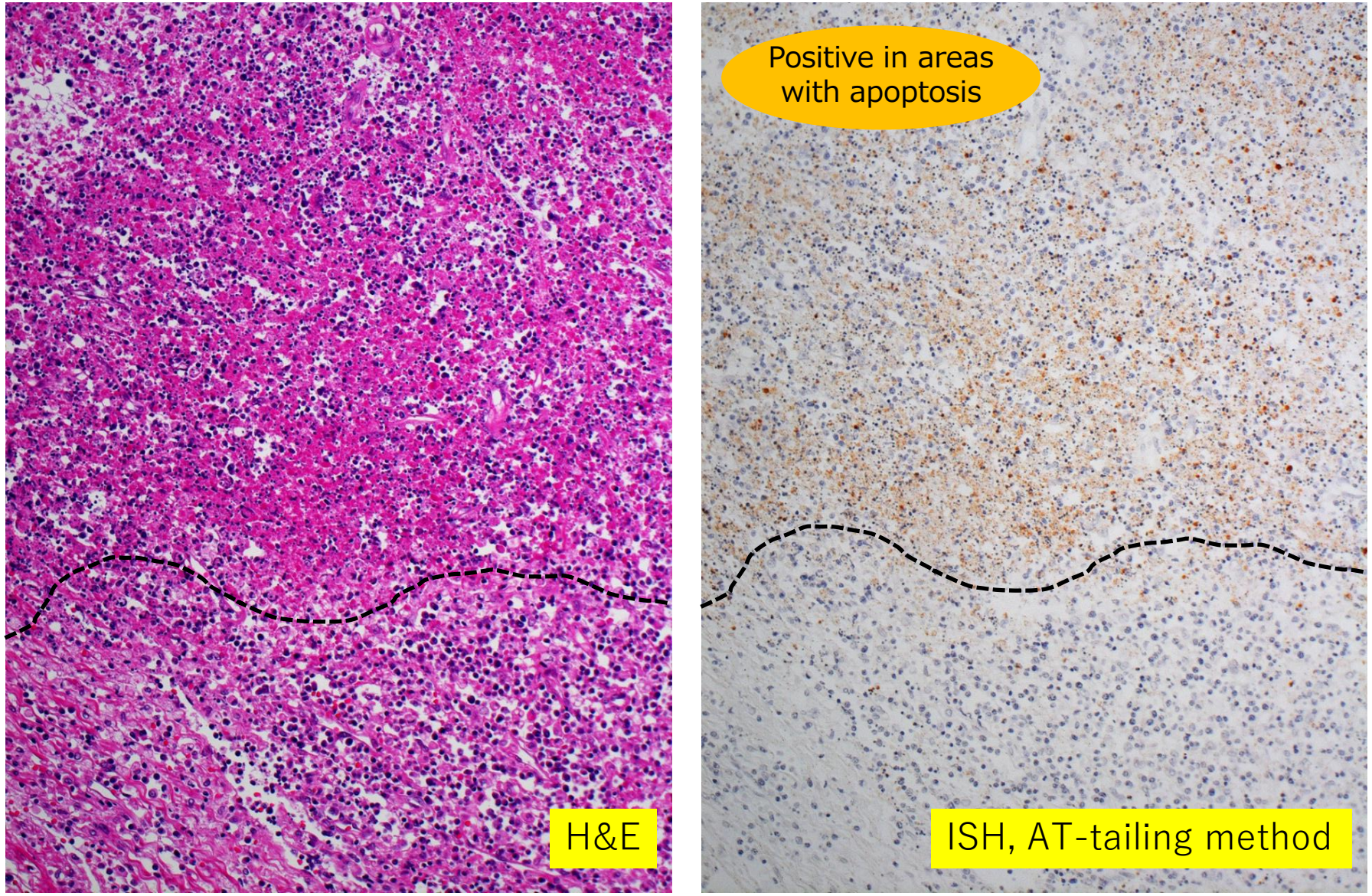


**Severe fever thrombocytopenia syndrome (SFTS)** in the autopsied lymph node. Left: H&E, right: *in situ* hybridization for SFTS virus (AT-tailing method). Positive signals (viral genomes) are clustered in the upper part of the lesion, where marked apoptotic death is observed.

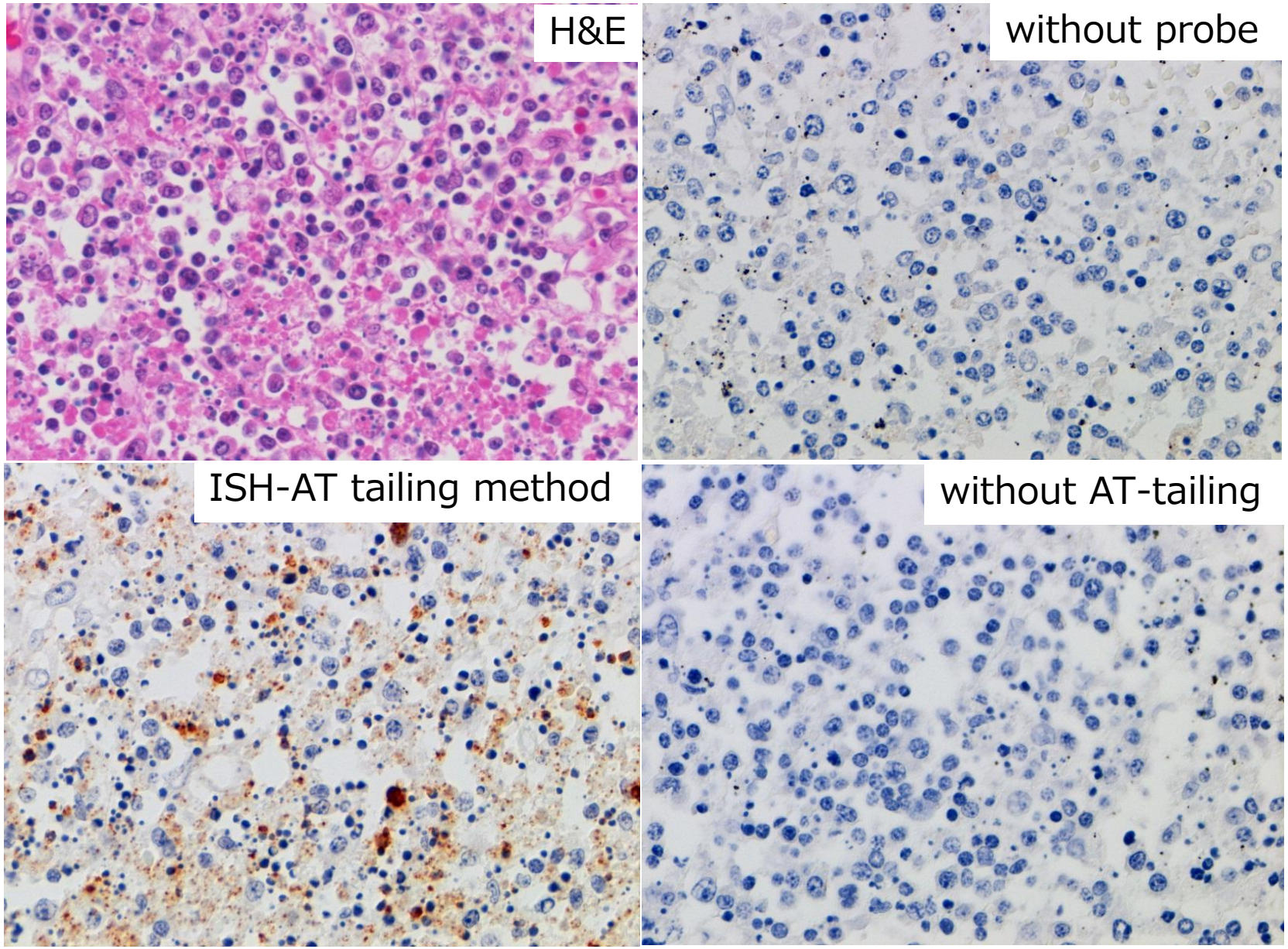


**Severe fever thrombocytopenia syndrome (SFTS)** in the autopsied lymph node. Positive ISH signals with AT-tailing method (SFTS viral genomes) are seen in the cytoplasm of macrophages with apoptotic bodies. Negative controls without probe or without AT-tailing give negative results.

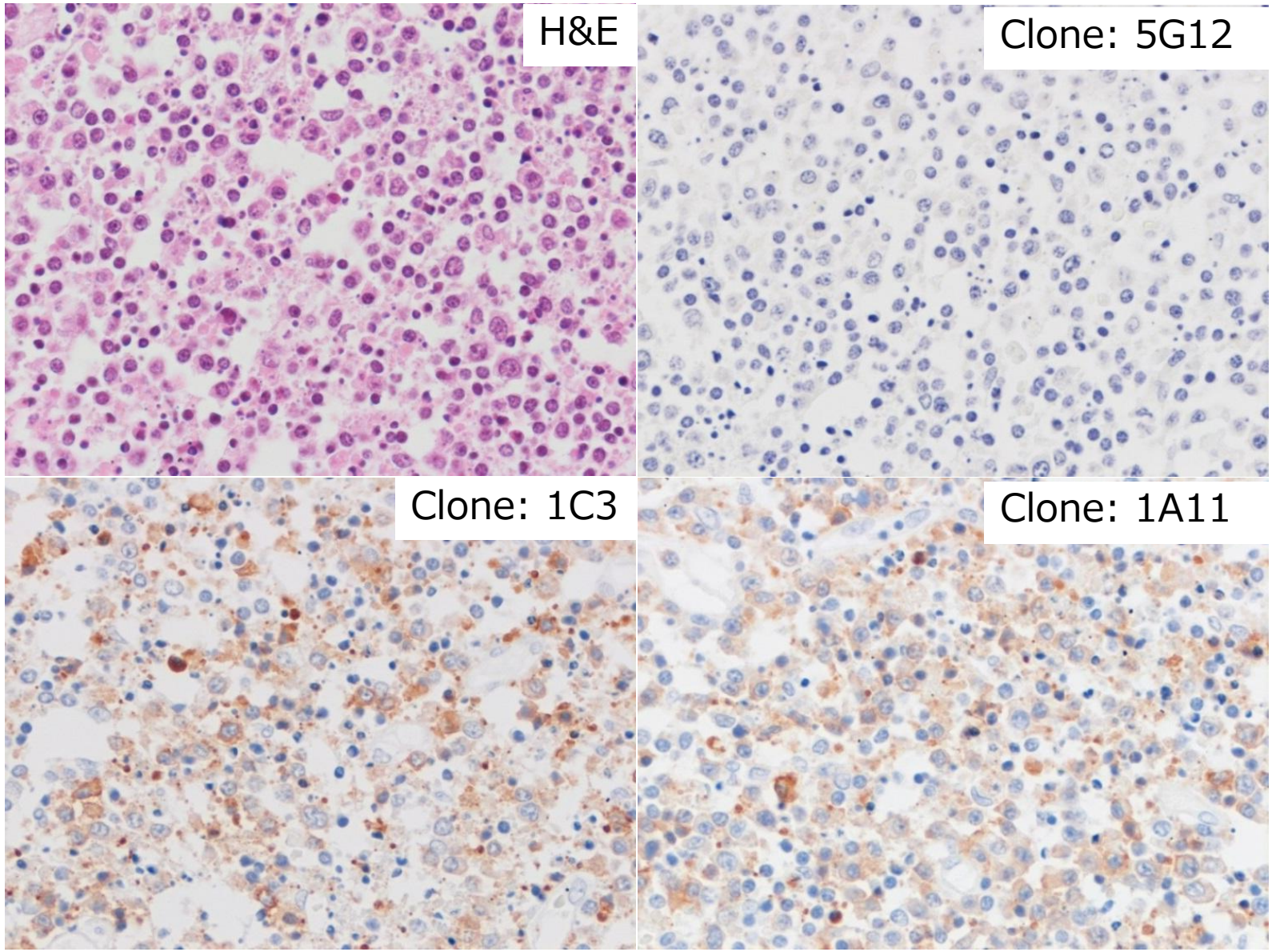


**Severe fever thrombocytwotopenia syndrome (SFTS)** in the autopsied lymph node. Positive immunohistochemical signals of SFTS viral antigens are seen in the cytoplasm of macrophages with apoptotic bodies. Two of three monoclonal antibodies (clones 1C3 and 1A11) give positive signals.

# Pre-embedding method for ISH at EM level

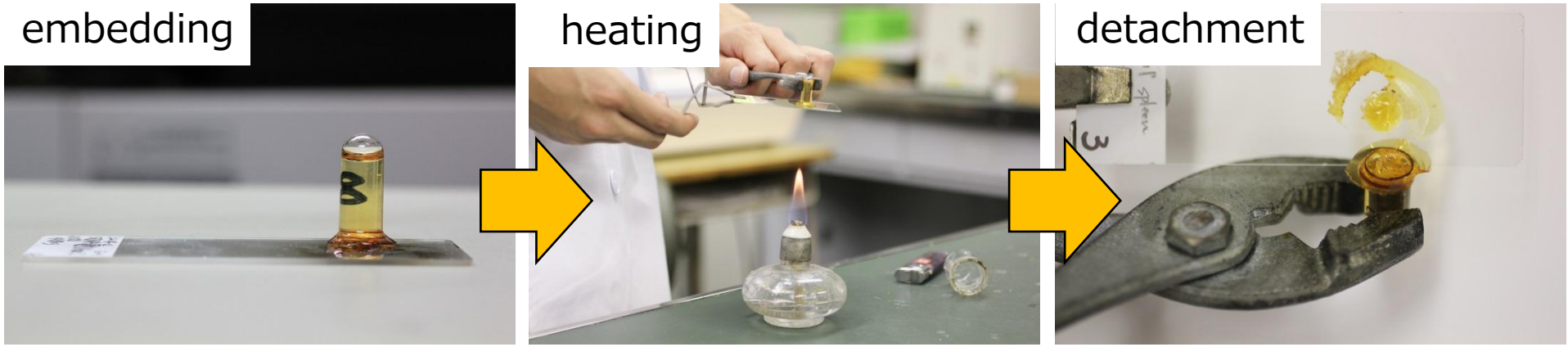


Both immunostaining and ISH require heating pretreatment to get signals. Therefore, the use of coating slides is indispensable.

| MBL TACAS | Muto Glass A | Muto Glass B | Muto Glass C | Muto Glass D |
|---|---|---|---|---|
| **5/5 (100%)** | 0/5 (0%) | 1/5 (20%) | 0/5 (0%) | 3/5 (60%) |

The Silane-coated slides (Muto's glass A-D) are resistant to detaching the stained sections. We have serious technical dilemma. TACAS slides can solve this reciprocal problem.

# ISH for SFTS virus at the EM level

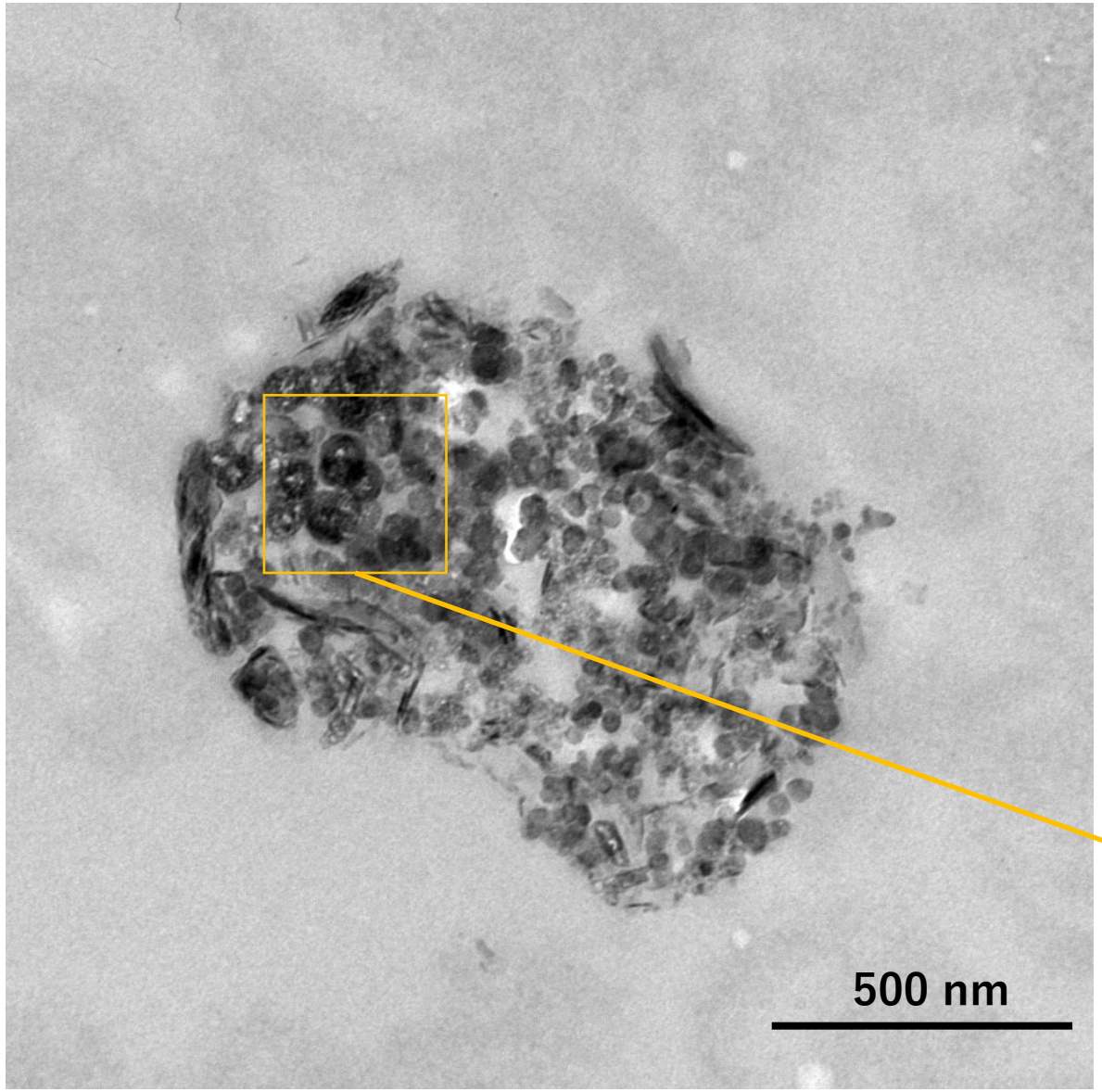


- The size of SFTS virus = 100 nm
- Site: lymph node (autopsy)
- Antisense cocktail probe used

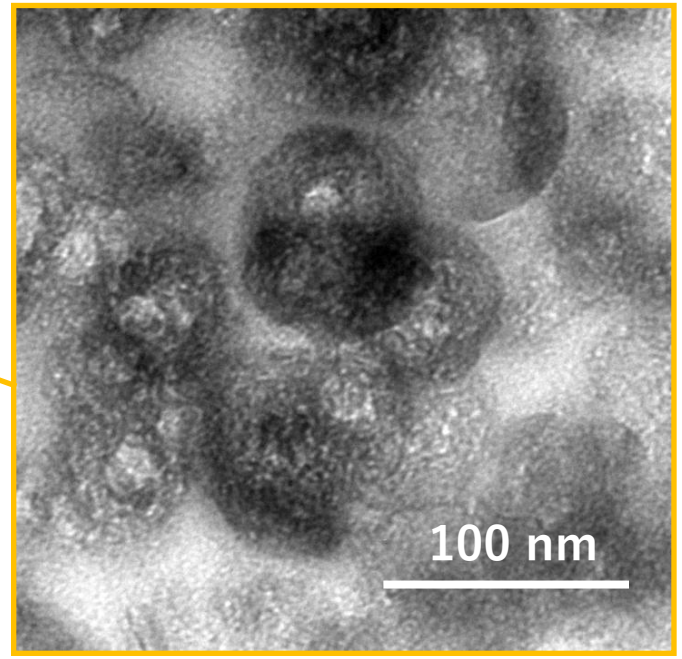

# Immunoelectron microscopy for SFTS virus

phagocytized red blood cell

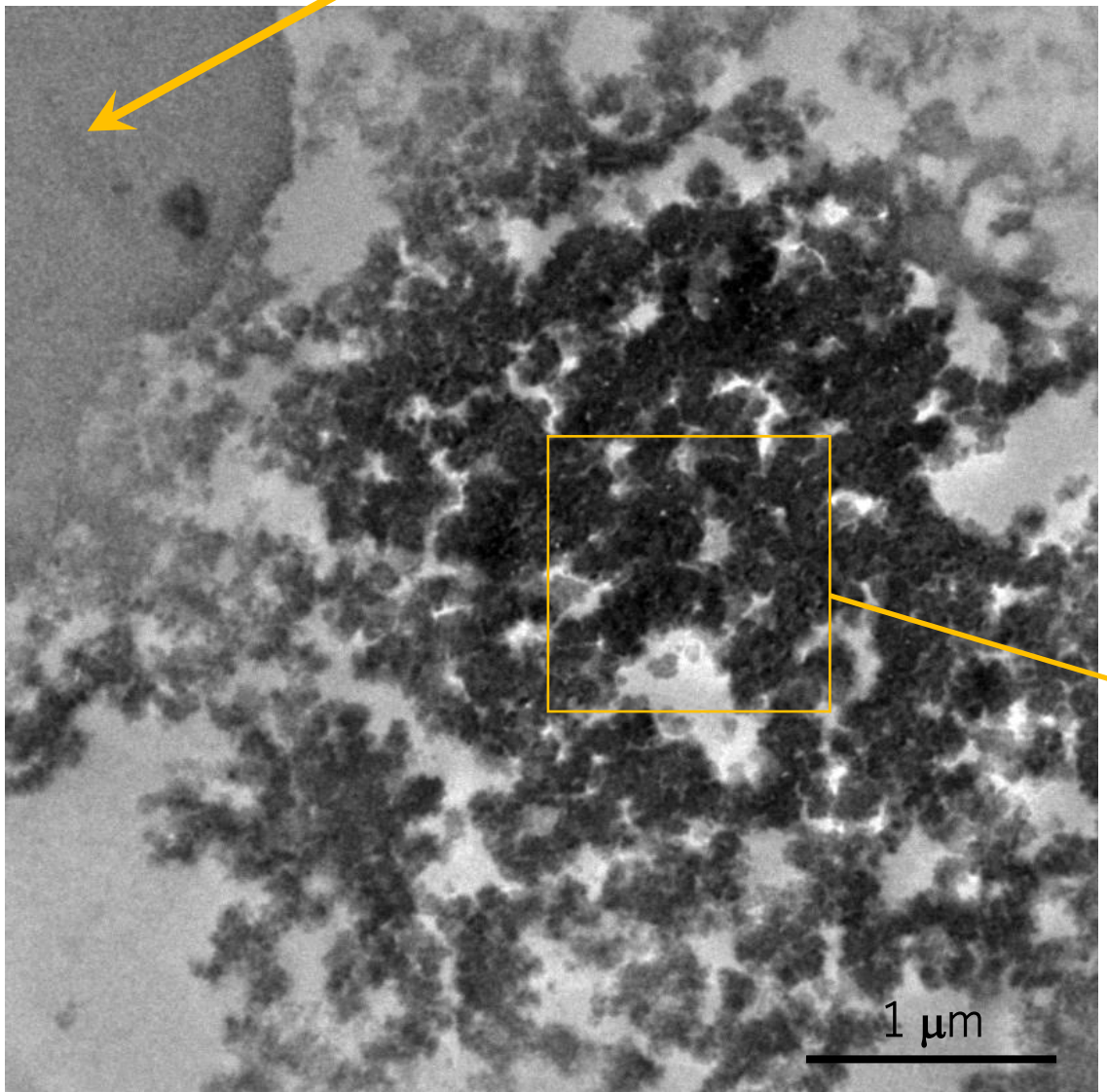


- The size of SFTS virus = 100 nm
- Site: spleen
- 1C3 monoclonal Ab used for the pre-embedding method

**Ref.**: Matsui T, et al. Coated glass slides TACAS are applicable to heat-assisted immunostaining and in situ hybridization at the electron microscopy level. Acta Histochem Cytochem 2015; 48(5): 153-157. doi: 10.1267/ahc.15012

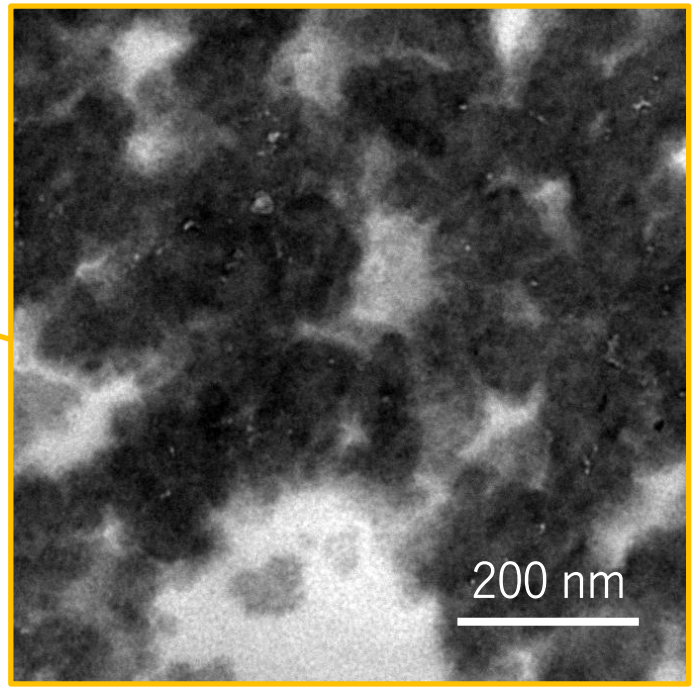

# Visualization of HPV antigen in formalin-fixed, paraffin-embedded sections-1

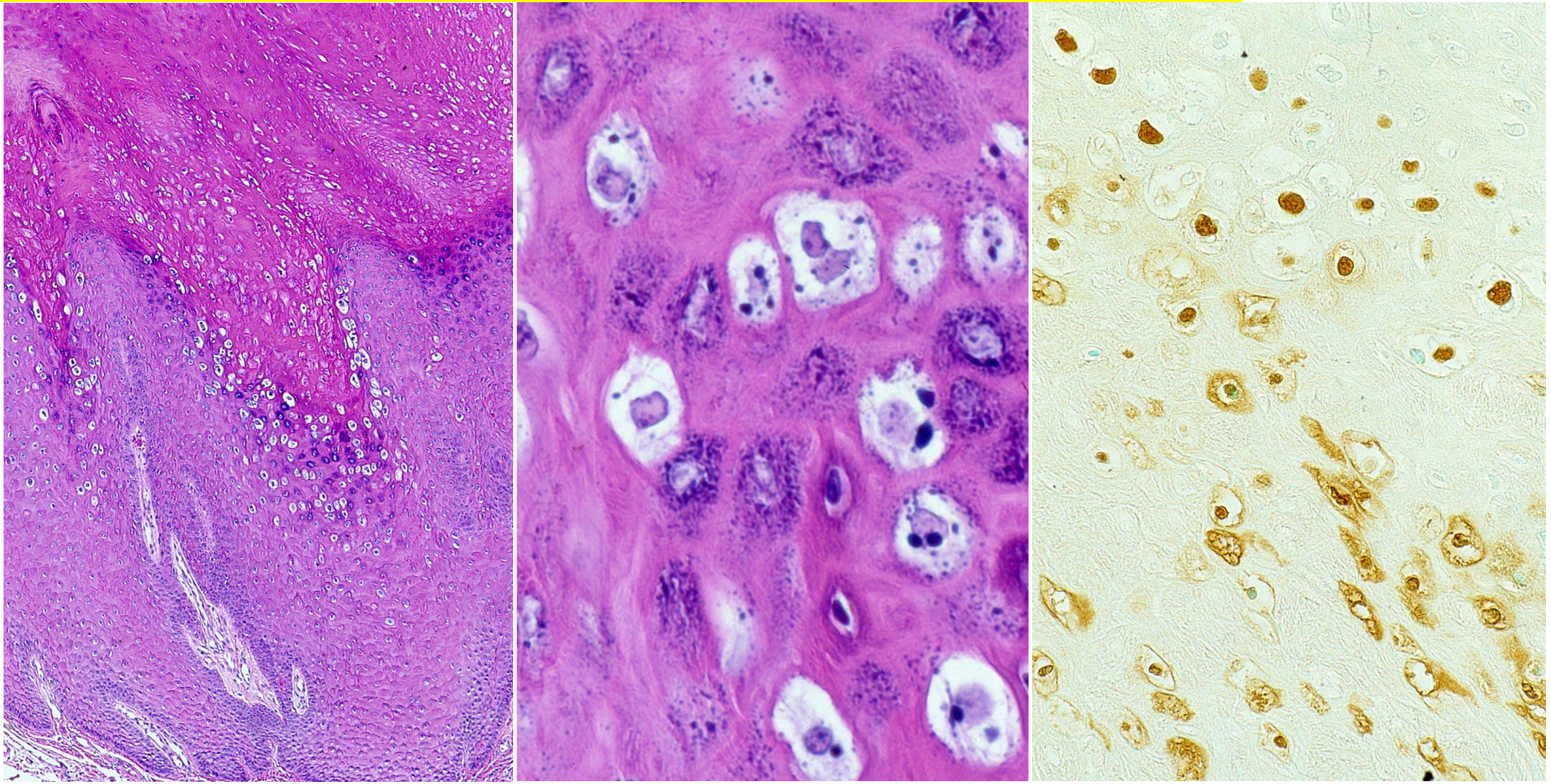

Verruca vulgaris (skin, H&E and immunostaining for HPV capsid antigens).
The thickened granular layer cells show koilocytic change with positivity for HPV capsid antigens.

# Visualization of HPV antigen in formalin-fixed, paraffin-embedded sections-2

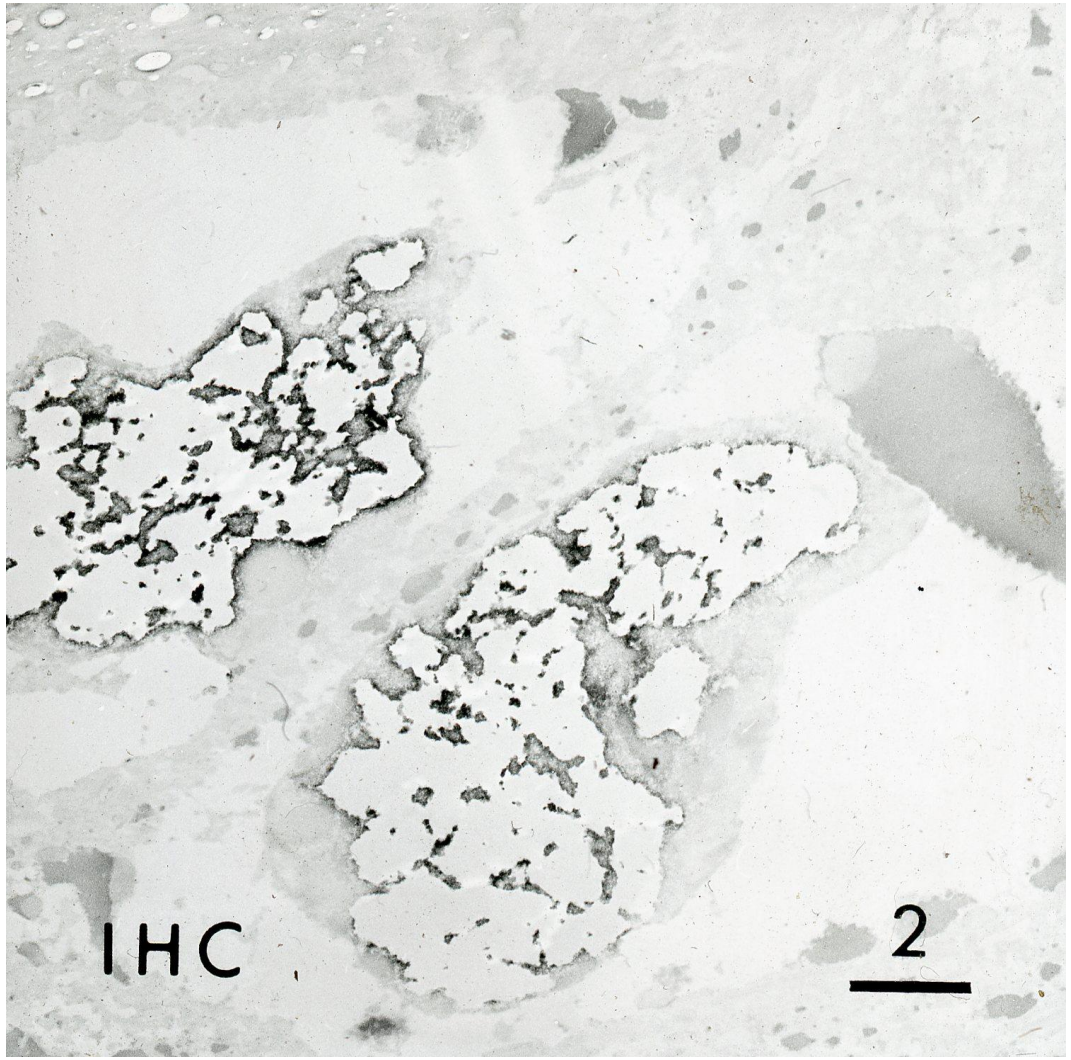


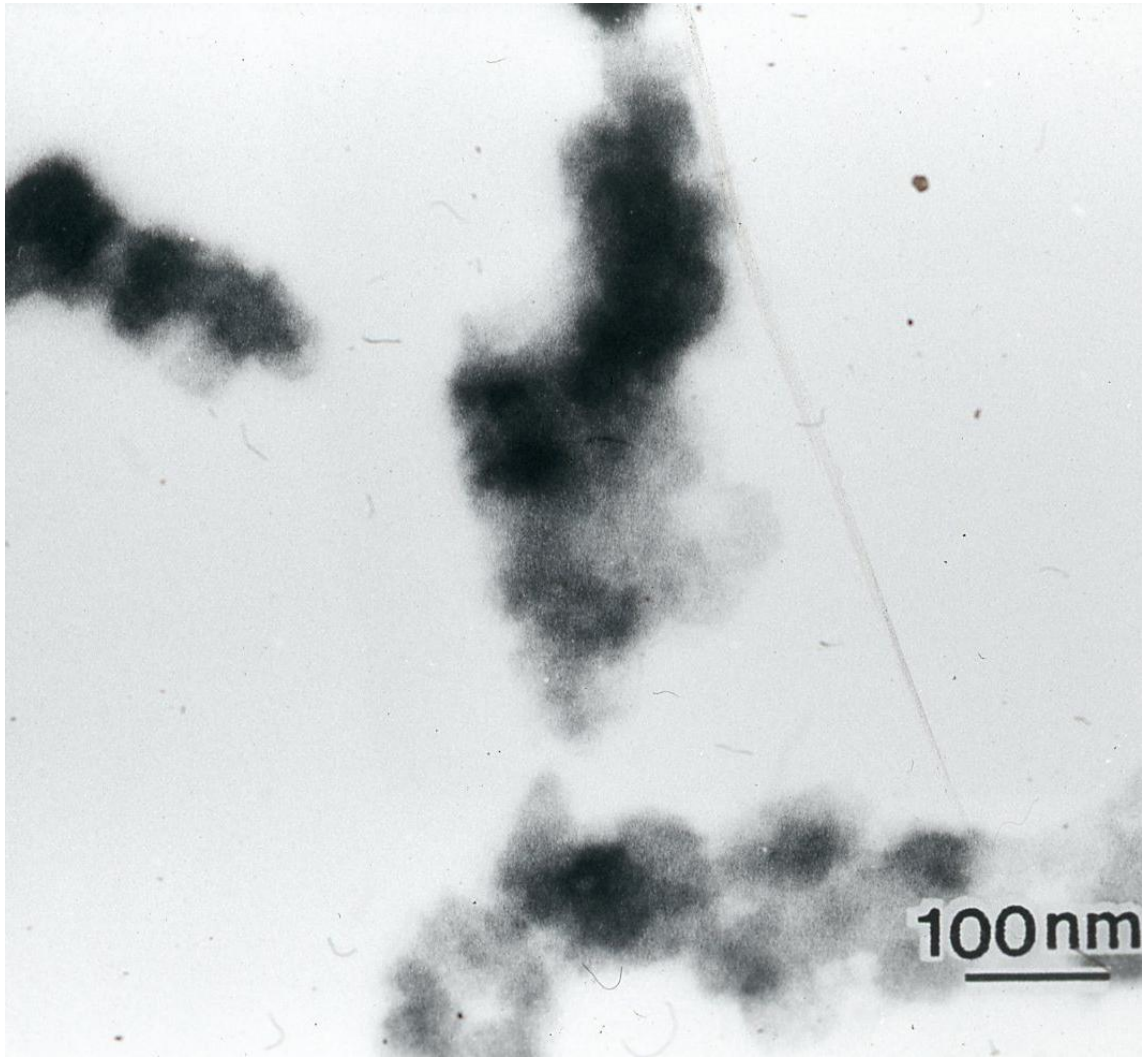


Immunoelectron microscopy for HPV capsid antigens using formalin-fixed, paraffin-embedded sections of verruca vulgaris. In the koilocytic nucleus seen in the granular layer with keratohyaline granules, viral particles measuring 50-60 nm are observed.

# Visualization of HPV genome in formalin-fixed, paraffin-embedded sections-1

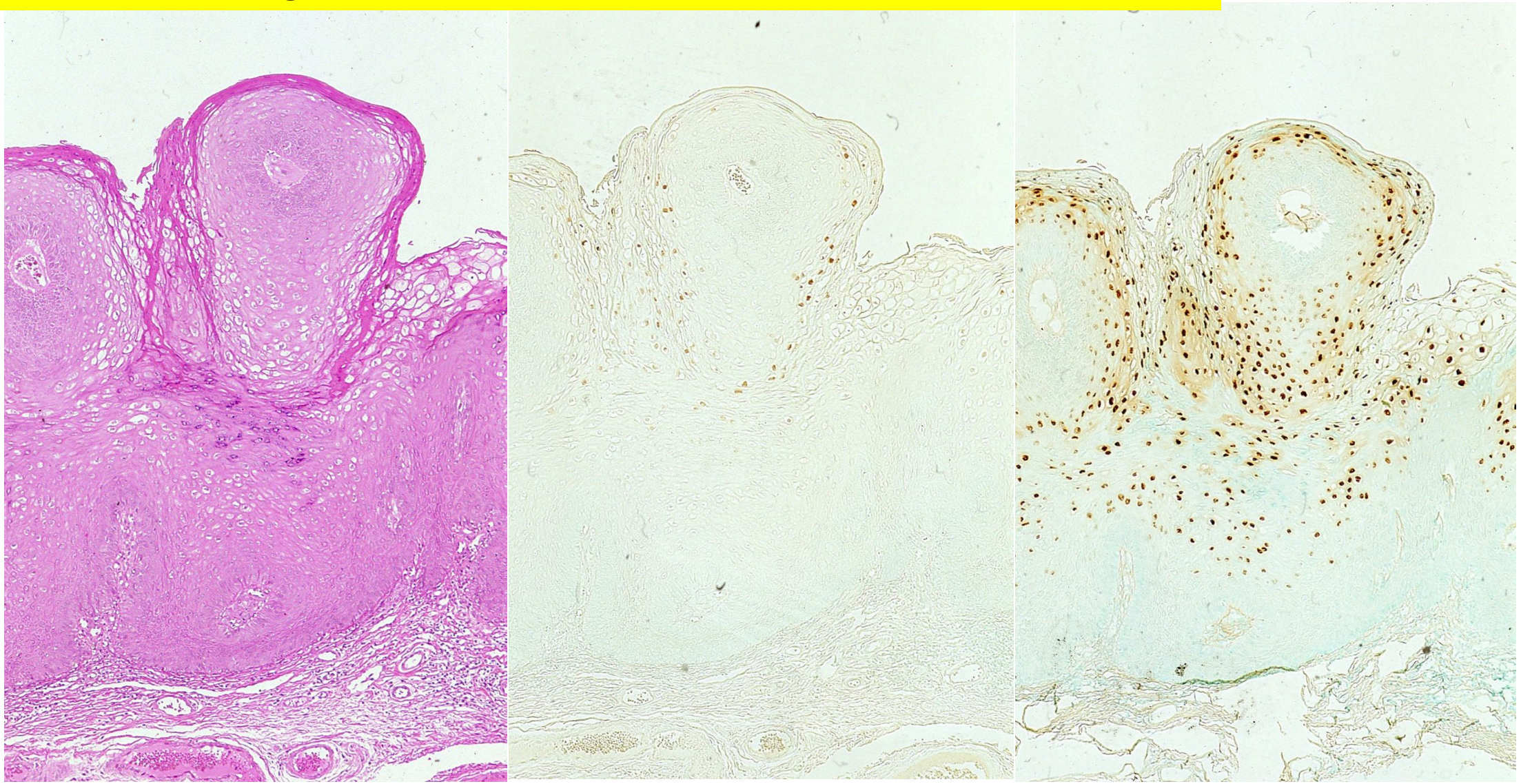

Condyloma acuminatum (left: H&E, center: immunostaining for HPV capsid antigens, right: ISH using wide-spectrum HPV probes). HPV capsid antigen is seen in part of the koilocytic nuclei, while more papillomatous keratinocytes are positive for HPV genome.

# Visualization of HPV genome in formalin-fixed, paraffin-embedded sections-2

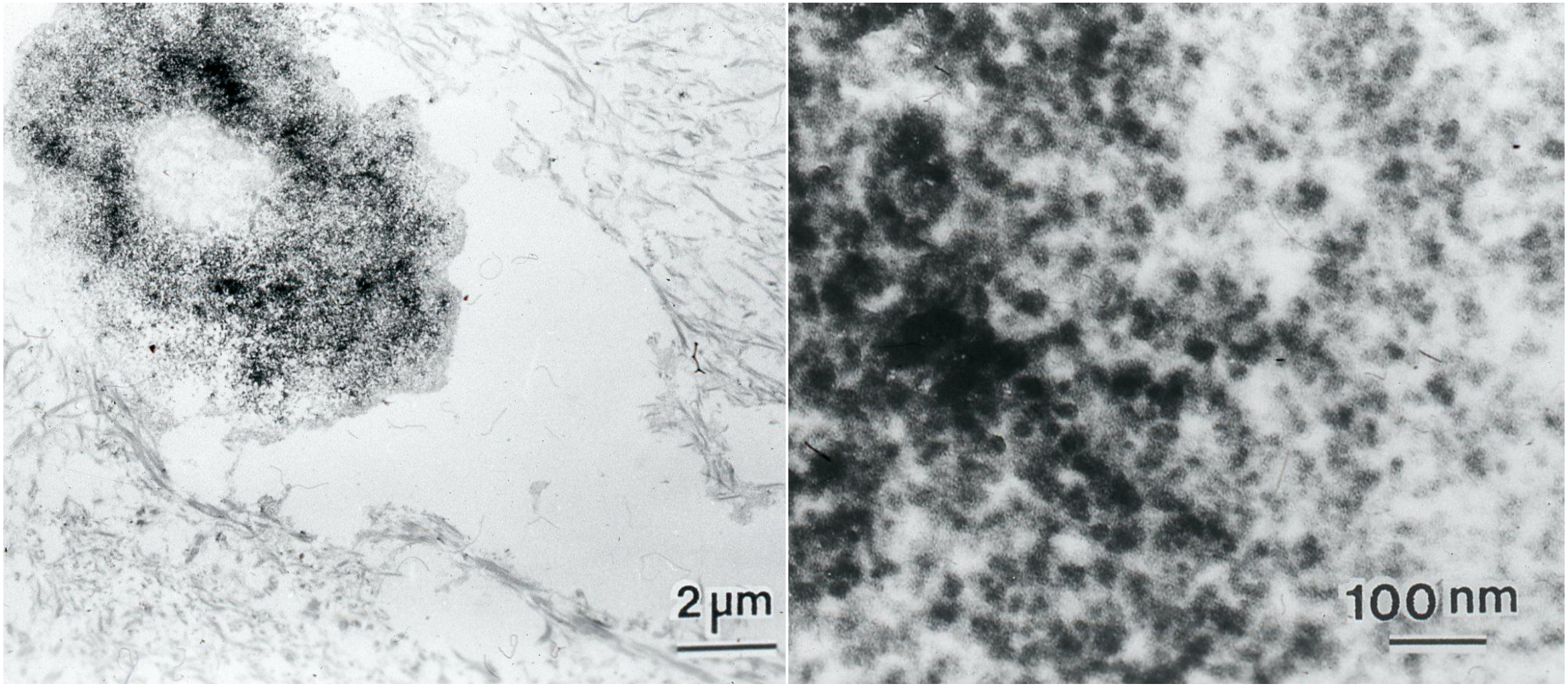


ISH signals at the EM level in condyloma acuminatum. Fine-particulated signals measuring 20 nm are observed in the nuclei, representing episomal viral DNA. This nucleus without viral particle formation is positive with ISH but negative for immunostaining.

# Visualization of HPV genome in formalin-fixed, paraffin-embedded sections-3

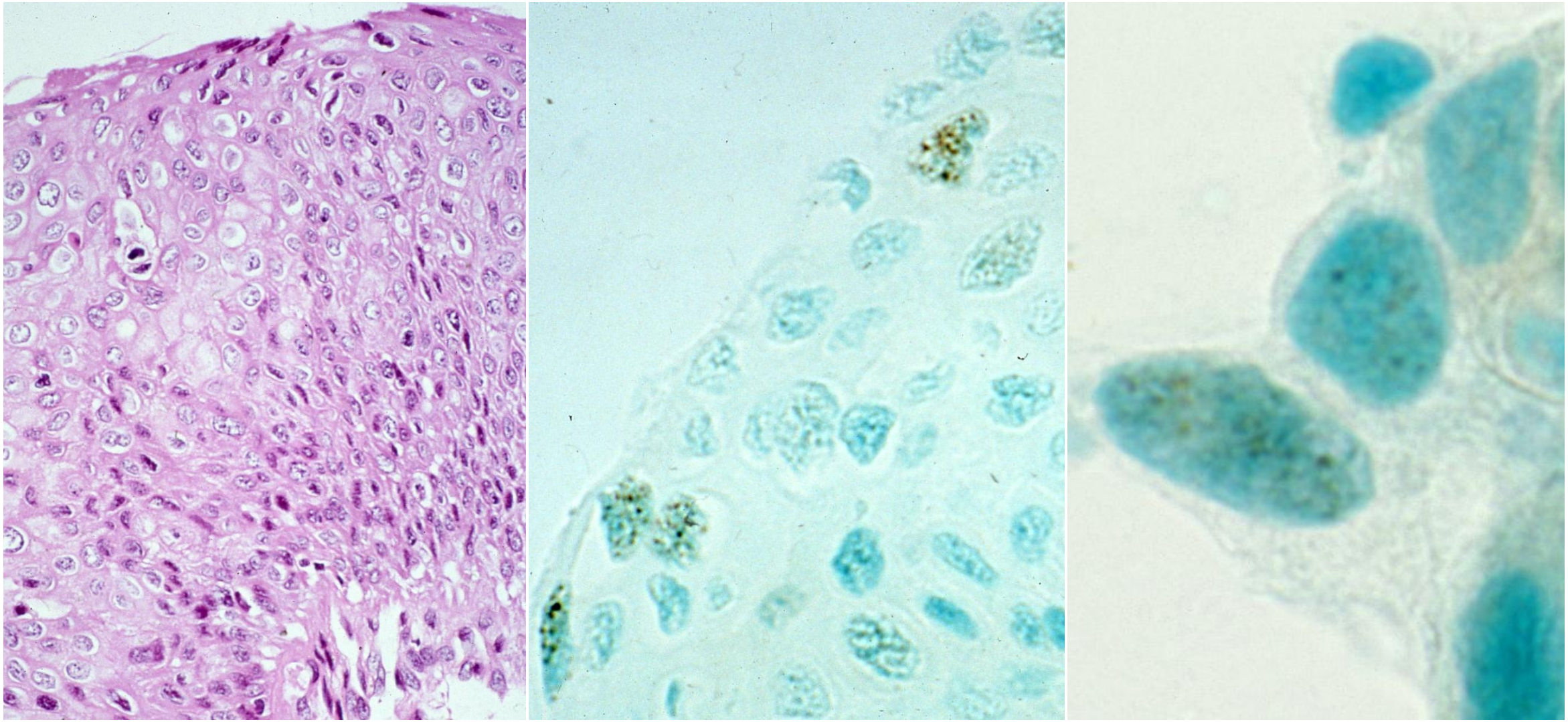

Severe dysplasia of the uterine cervix. Left: H&E, center: ISH for HPV genome, right: ISH for HPV genome in cytology specimen. Wide-spectrum (cocktail) HPV probes are used. Dotted positive signals are seen in the dysplastic nuclei.

# Visualization of HPV genome in formalin-fixed, paraffin-embedded sections-4

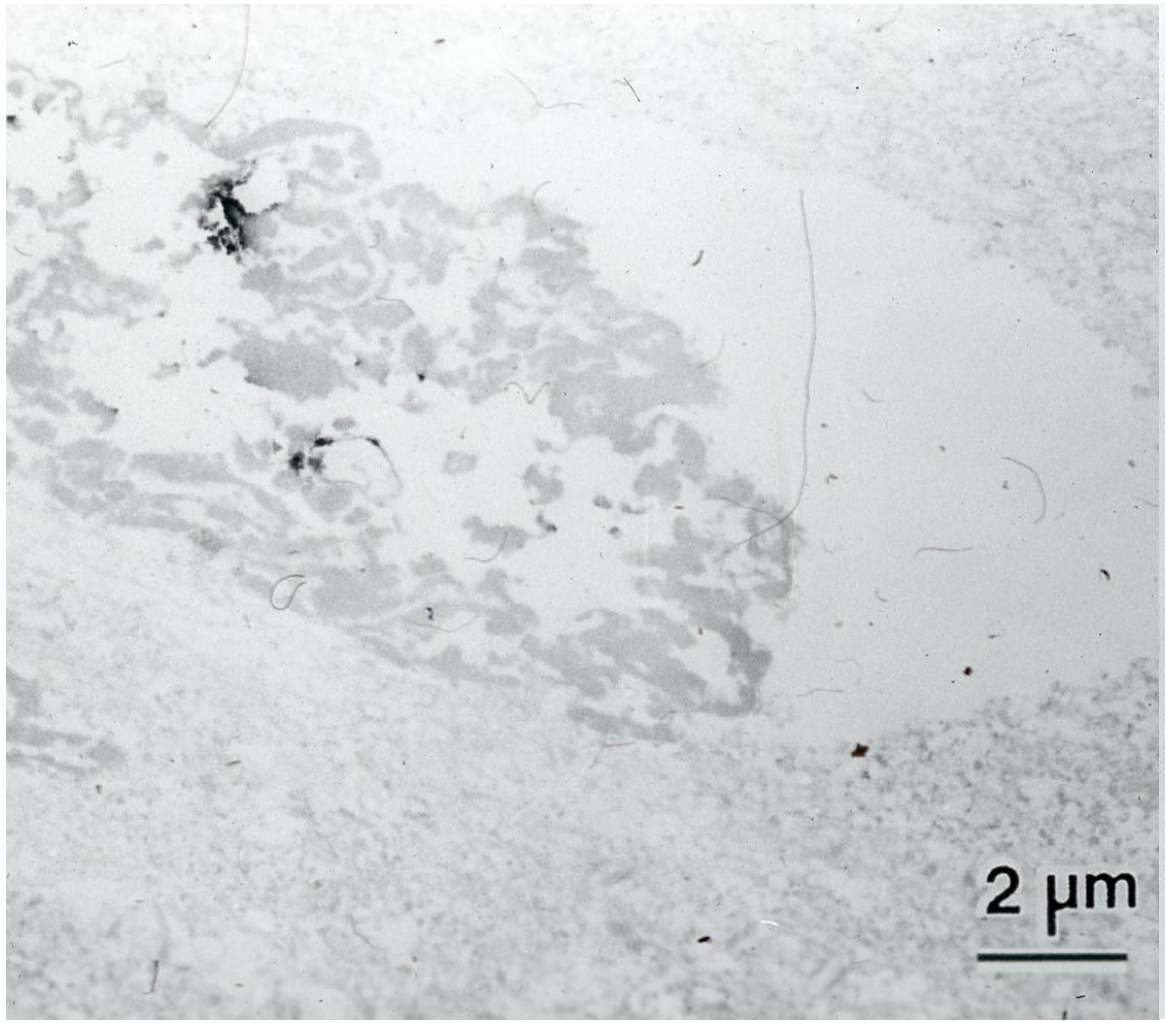


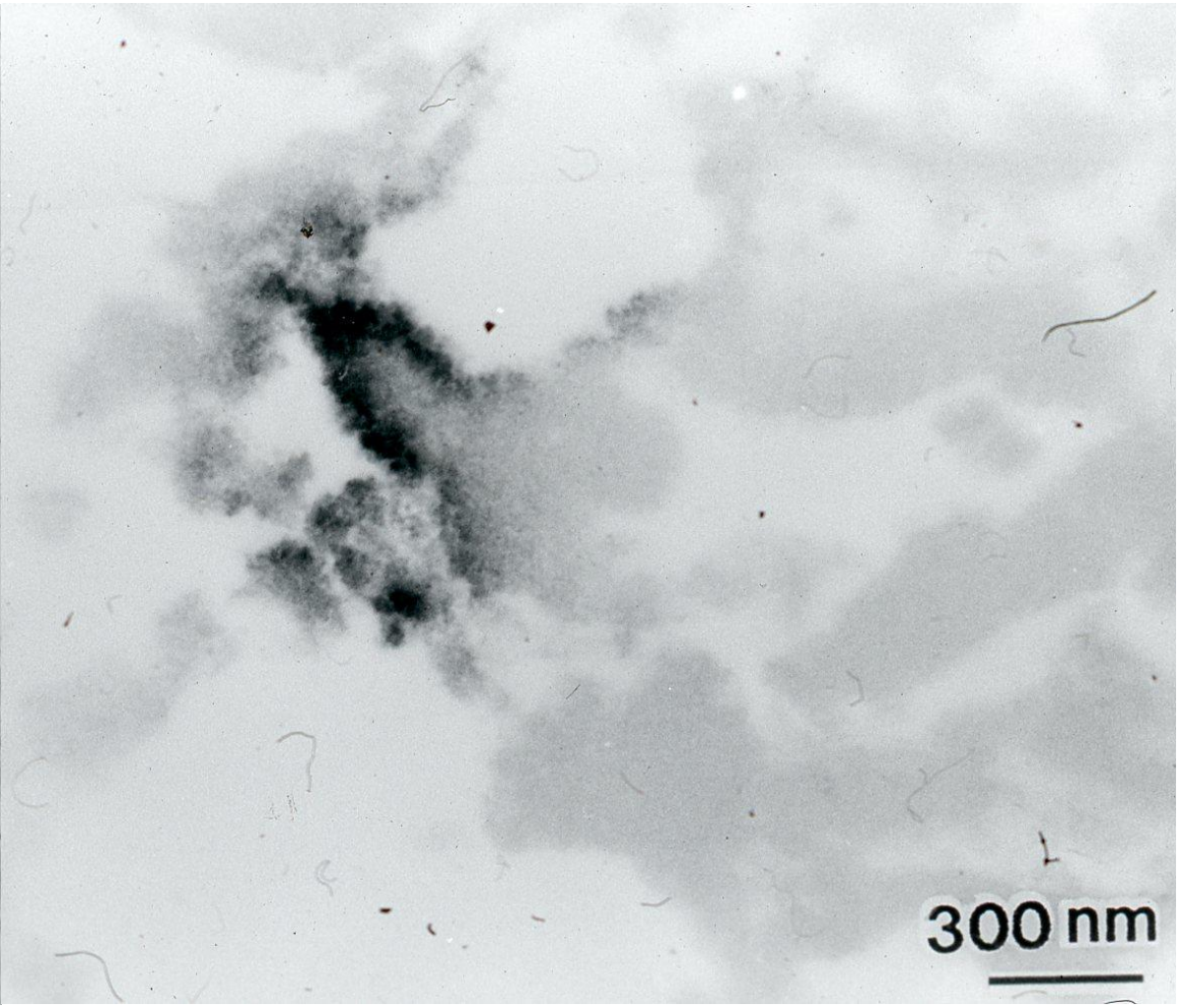


ISH at the EM level in severe dysplasia of the uterine cervix, using formalin-fixed, paraffin-embedded sections. The positive signals are seen on a part of chromatin with a dotted pattern. This represents the integration of viral DNA into the genome of the host cell. **Ref.**: Tsutsumi Y, et al. Ultrastructural visualization of human papillomavirus DNA in verrucous and precancerous squamous lesions. Acta Pathol Jpn 1991; 41(10): 757-762. doi: 10.1111/j.1440-1827.1991.tb03348.x